

2015

# The role of bone morphogenetic protein 2 in SMA-directed angiogenesis during distraction osteogenesis

---

<https://hdl.handle.net/2144/16261>

*Boston University*

BOSTON UNIVERSITY  
SCHOOL OF MEDICINE

Thesis

**THE ROLE OF BONE MORPHOGENETIC PROTEIN 2 IN SMA-DIRECTED  
ANGIOGENESIS DURING DISTRACTION OSTEOGENESIS**

by

**THOMAS W. CHENG**

B.S., Johns Hopkins University, 2013

Submitted in partial fulfillment of the  
requirements for the degree of  
Master of Science

2015

© 2015 by  
THOMAS W. CHENG  
All rights reserved

Approved by

First Reader

---

Dr. Louis C. Gerstenfeld, Ph.D.  
Professor, Department of Orthopaedic Surgery

Second Reader

---

Dr. Beth Bragdon, Ph.D.  
Postdoctoral Research Fellow, Department of Orthopaedic Surgery

## **ACKNOWLEDGMENTS**

I will like to thank my family for their support. I will like to express special appreciation to Dr. Gerstenfeld and Dr. Bragdon for giving me the opportunity to conduct research in the laboratory and being close mentors throughout this project.

**THE ROLE OF BONE MORPHOGENETIC PROTEIN 2 IN SMA-DIRECTED  
ANGIOGENESIS DURING DISTRACTION OSTEOGENESIS**

**THOMAS W. CHENG**

**ABSTRACT**

Bone is one of the few organs capable of regeneration after a substantial injury. As the bone heals itself after trauma, the coupling of angiogenesis to osteogenesis is crucial for the restoration of the skeletal tissue. In prior studies we have shown that Bone Morphogenetic Protein 2 (BMP2), a potent agonist for skeletal formation is expressed by vessels making it a prime candidate that links the morphogenesis of the two tissues. To investigate the role of BMP2 in the coordination of vessel and bone formation, we used a tamoxifen inducible Smooth Muscle Actin (SMA) promoter that conditionally expresses Cre recombinases crossed with a BMP2 floxed mouse in order to conditionally delete the BMP2 gene in smooth muscle actin (SMA) expressing cells. Using the mouse femur as our model for bone regeneration, we performed a surgical technique called distraction osteogenesis (DO) where an osteotomy is created followed by distraction or a gradual separation of the two pieces of bone. This primarily promotes intramembranous ossification at the osteotomy site by mechanical stimulation. Tamoxifen treatment started at day 6 and continued throughout the experiment. At post-operative days 3, 7, 12, 17, 24, and 31, we analyzed the bone and vessel formation by plain X-ray, micro-computed tomography ( $\mu$ CT) and vascular contrast enhanced  $\mu$ CT, and quantitative polymerase

chain reaction (qPCR) of selective genes. We assessed both the femur and surrounding tissue to obtain qualitative and quantitative assessments for skeletal and vascular formation. Our results demonstrated that the deletion of BMP2 in vascular tissue resulted in a reduction of angiogenesis *in vivo* followed by a decrease in skeletal tissue development.

## TABLE OF CONTENTS

TITLE.....	i
COPYRIGHT PAGE.....	ii
READER APPROVAL PAGE.....	iii
ACKNOWLEDGMENTS .....	iv
ABSTRACT.....	v
TABLE OF CONTENTS.....	vii
LIST OF TABLES .....	x
LIST OF FIGURES .....	xi
LIST OF ABBREVIATIONS.....	xiii
INTRODUCTION .....	1
<i>Bone Cells</i> .....	1
<i>Modes of Bone Formation</i> .....	1
<i>Fracture Statistics</i> .....	2
<i>Distraction Osteogenesis</i> .....	3
<i>Bone Morphogenetic Proteins</i> .....	6
<i>Angiogenesis</i> .....	7
<i>Cre-loxP System</i> .....	9
<i>Experimental Aims</i> .....	11



MATERIALS AND METHODS.....	13
<i>Animal Model</i> .....	13
<i>List of Common Reagents Used</i> .....	14
<i>Surgical Procedure for Distraction Osteogenesis</i> .....	15
<i>Distraction Procedure</i> .....	16
<i>Control Injections</i> .....	16
<i>Tamoxifen Injections</i> .....	17
<i>Harvest Procedure</i> .....	17
<i>RNA Extraction</i> .....	18
<i>cDNA Procedure</i> .....	20
<i>Quantitative Polymerase Chain Reaction (qPCR)</i> .....	21
<i>Primers used for Real Time Polymerase Chain Reaction (RT-PCR)</i> .....	21
<i>Micro-Computed Tomography (micro-CT) for Bone Evaluation</i> .....	23
<i>Vessel Analysis</i> .....	24
Vessel Perfusion.....	24
Micro-Computed Tomography (micro-CT) for Vessel Evaluation.....	26
Decalcification for Vessel Scanning.....	26
<i>Statistical Methods</i> .....	27
RESULTS.....	28
<i>qPCR for Distraction Gap</i> .....	28
<i>qPCR for Muscle</i> .....	34
<i>X-Ray</i> .....	36

<i>μCT Bone Evaluation</i> .....	39
<i>μCT Microfil Vessel Perfusion</i> .....	43
<i>μCT Barium Vessel Perfusion</i> .....	46
DISCUSSION .....	50
<i>Future Goals</i> .....	52
REFERENCES .....	54
CURRICULUM VITAE.....	59

## LIST OF TABLES

Table 1: Enrollment of animals and their uses.....	14
Table 2: Common reagents and equipment used for the study.....	15
Table 3: Genes related to bone production, bone resorption, chondrogenesis, and angiogenesis.....	23

## LIST OF FIGURES

Figure 1: The role of Bone Morphogenetic Proteins (BMPs) for bone formation .....	4
Figure 2: Visual Summary of Distraction Osteogenesis Phases.....	5
Figure 3: Distraction Osteogenesis Stages and Their Biological Processes.....	6
Figure 4: Cre-lox system.....	10
Figure 5: Tissue-specific Cre- <i>loxP</i> system.....	10
Figure 6: Experimental Timeline.....	11
Figure 7: Distraction Gap qPCR Results for Bone Production.....	31
Figure 8: Distraction Gap qPCR Results for Bone Resorption.....	32
Figure 9: Distraction Gap qPCR Results for Chondrogenesis.....	33
Figure 10: Distraction Gap qPCR Results for Angiogenesis.....	34
Figure 11: Muscle qPCR Results for Osteogenesis .....	35
Figure 12: Muscle qPCR Results for Angiogenesis .....	36
Figure 13: DO X-ray Results.....	38
Figure 14: Day 31 2D $\mu$ CT Results for Bone Evaluation.....	39
Figure 15: $\mu$ CT Bone Evaluation for Control.....	41
Figure 16: $\mu$ CT Bone Evaluation for BMP2 Knockout.....	42
Figure 17: Day 31 2D $\mu$ CT Results for Vessel Perfusion.....	44
Figure 18: Day 31 3D Pre-decalcified $\mu$ CT Results.....	45
Figure 19: Day 31 3D Post-decalcified $\mu$ CT Results.....	46
Figure 20: Barium Perfused Samples.....	47
Figure 21: Comparison of Barium to Microfil.....	48

Figure 22: Barium Vessel Perfusion for Control Versus BMP2 Knockout..... 49

## LIST OF ABBREVIATIONS

Ba .....	Barium
BMP2 .....	Bone Morphogenetic Protein 2
CDC .....	Center for Disease Control and Prevention
DO.....	Distraction Osteogenesis
DNA.....	Deoxyribonucleic acid
EDTA.....	Ethylenediaminetetraacetic acid
HCl.....	Hydrochloric acid
IP.....	Intraperitoneal Injection
qPCR.....	Quantitative Polymerase Chain Reaction
RNA .....	Ribonucleic acid
RBE.....	Recombinase binding element
TGF $\beta$ .....	Transforming growth factor beta
v/w.....	volume per weight
VEGFs.....	Vascular Endothelial Growth Factor
w/v.....	weight per volume
$\mu$ CT.....	Micro-Computed Tomography

## **INTRODUCTION**

### ***Bone Cells***

There are three main cell types that contribute to bone. They are called the osteoblasts, osteocytes, and osteoclasts (Mescher, 2013). The osteoblasts become osteocytes when the bone matrix, made of mainly type I collagen and calcium and phosphate crystals in the form of hydroxyapatite, that they produce eventually surrounds and traps themselves in a cavity called a lacunae (Takayanagi, 2007). Osteoblasts have proliferative potential and are associated primarily with the synthesis of new bone extracellular matrix whereas the osteocytes are non-proliferative and are associated with the regulatory processes of mineral metabolism and mechano-signal transduction (Clarke, 2008; Mescher, 2013; Takayanagi, 2007). The main role of the osteoblasts and osteocytes are anabolic and regulatory forming bone tissues whereas the osteoclasts are catabolic and resorb bone (Clarke, 2008).

### ***Modes of Bone Formation***

Bone formation occurs through two process: endochondral and intramembranous osteogenesis. In endochondral ossification, cartilage tissue is first formed and then replaced with bone. There are various stages for this process starting with the recruitment of mesenchymal cells that then undergo differentiation into chondrocytes. The chondrocytes then undergo proliferation and start to secrete cartilage which is the template for bone to replace (Mackie et al., 2008). The chondrocytes then cease proliferation and become hypertrophic (Mackie et al., 2008). At this stage, the

hypertrophic chondrocytes add collagen X to the extracellular matrix to allow for mineralization (Mackie et al., 2008). Blood vessels penetrate the cartilage to allow the cartilage to be mineralized by osteoblasts and the hypertrophic chondrocytes undergo apoptosis. Also at this time, the cartilage is reabsorbed by osteoclasts (Mackie et al., 2008). This is seen in long bones such as a developing femur as it lengthens and matures. In intramembranous ossification involves direct bone formation from mesenchymal tissue without a cartilage base (Percival et al., 2013). It is shown in prior studies that Bone Morphogenetic Proteins (BMPs) are vital for intramembranous osteogenesis (Percival et al., 2013). This characteristic process occurs in bones such as flat bones located in the mandibular and the skull (Aronson, 1994).

### ***Fracture Statistics***

Fractures occur when the bone is subjected to trauma which results in a break in the bone matrix (Marsell & Einhorn, 2011; Mescher, 2013). According to the CDC, in 2010 there were 43 incidents of fractures overall for every 1,000 people, with people over age 75 having the highest rate of 115 per 1,000 (CDC, 2013). These staggering statistics not only results in expensive medical costs for treatment but also the medical expenses that follow complications. The total cost of male and female medical fees combined was \$349 million in 2005 (CDC, 2013). It would be beneficial to understand the underlying mechanisms of bone repair in order to manipulate and decrease patient recovery time.



## *Distraction Osteogenesis*

Distraction osteogenesis (DO) is a surgical technique used to “apply controlled traction” to enhance the healing process and remodeling of bone (Natu et al., 2014). First introduced by Dr. Ilizarov in 1951, DO has been involved in various complicated orthopaedic cases such as mandibular defects, limb lengthening, and other craniofacial deformities (Ai-Aql, Alagl, Graves, Gerstenfeld, & Einhorn, 2008; Aronson, 1994; Makhdom & Hamdy, 2013). It is thought the physical stimulation caused by the mechanical forces during DO activates tissue growth (Natu et al., 2014).

When applied to animal models, this surgical technique provides a unique opportunity for this study to investigate how BMP2 directs bone regeneration by measuring the temporal molecular events during bone regeneration. It differs from fractures in that the response is primarily bone driven lacking the development of extensive amount of cartilage tissue which is typical of the endochondral bone formation process associated with a fracture model. This allows us to be able to clearly see mechanisms that are related to intramembranous formation.

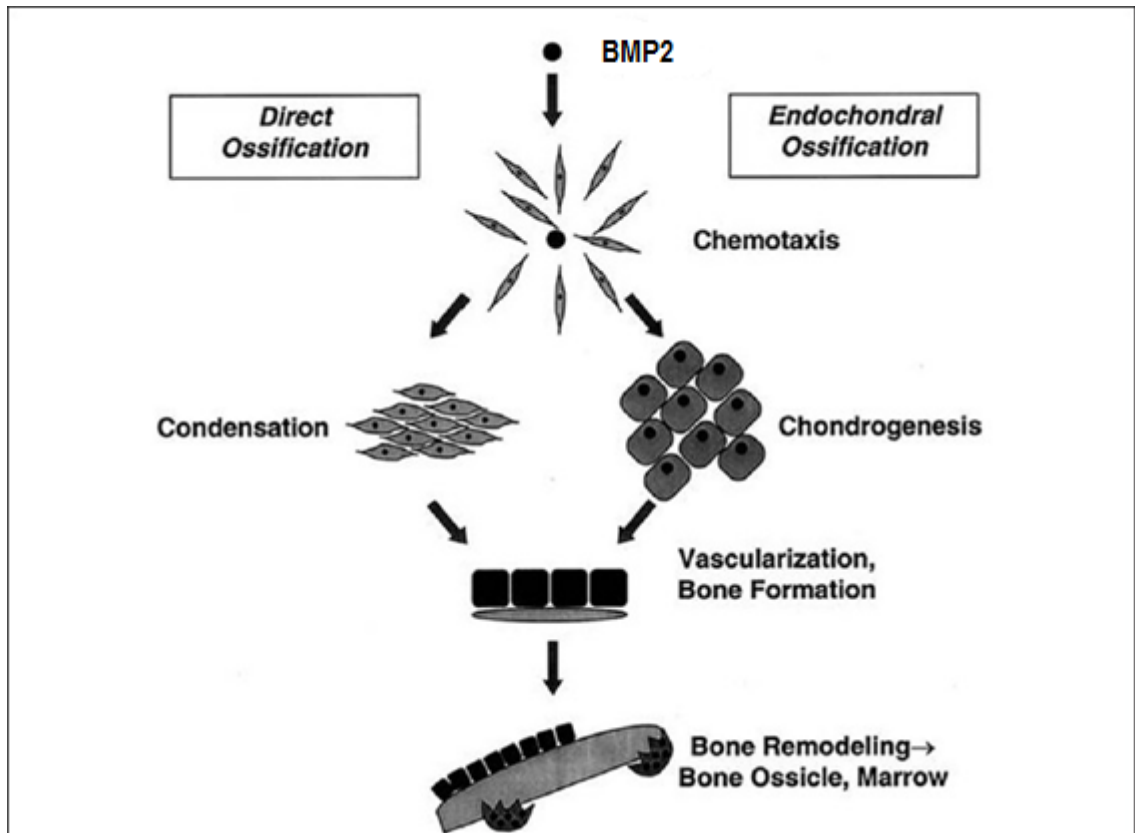


**Figure 1: The role of Bone Morphogenetic Proteins (BMPs) for bone formation.** Process of bone healing once BMP2 has been placed at a specific site. Figure taken and adapted from Jain et al., 2013.

The DO procedure is separated into 3 phases: latency, distraction, and consolidation which is shown in Figure 2 (Ai-Aql et al., 2008; Natu et al., 2014). During the latency phase, a hematoma is formed followed by inflammation and recruitment of mesenchymal stem cells as indicated by the presence of Il-1 and Il-6 which activate T cells (Dienz & Rincon, 2010; Lichtman et al., 1988). At the end of the latency phase, a callus is formed as first indicated by Sox9 then Acan then Col10a (Bi et al., 1999; Wigner et al., 2013). During the distraction phase, this callus is then stretched by the distraction device resulting in physical stimulation and further ossification as indicated by elevated of BMP2, the potent agonist for bone formation. At this stage, osteoblasts are actively

recruited to the site (Bais et al., 2009). Furthermore, vascular endothelial growth factors (VEGFs) especially VegfA are elevated to promote vessel formation to nourish the callous. In the consolidation phase, not shown in Figure 3, the bone is remodeled by the osteoclasts as shown by presence of RANKL and Cathepsin K (Takayanagi, 2007). Also, during the consolidation phase, serum markers for bone resorption has been identified as Trap5b (Shidara et al., 2008). As shown in Figure 3, there are various other biological processes with their accompanying cytokines and growth factors within each DO phase.

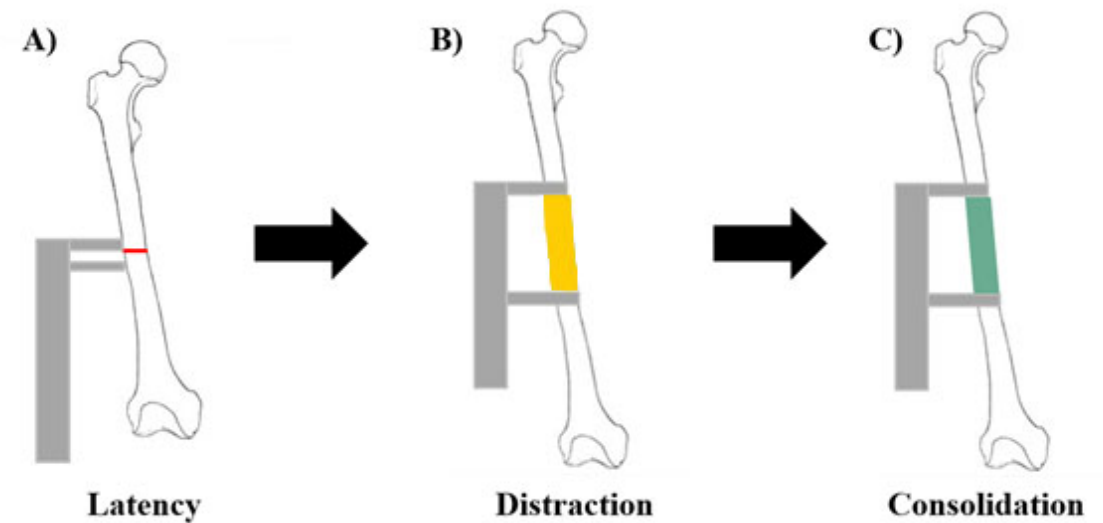


**Figure 2: Visual Summary of Distraction Osteogenesis Phases.** The gray object represents the distraction device. (A) Latency phase of distraction osteogenesis. The red line indicates a transverse osteotomy (B) Distraction phase. The yellow parallelogram represents a formed callus (C) Consolidation. The green parallelogram represents new bone formation.

Stage of Distraction Osteogenesis	Biological Processes	Expression of Signaling Molecules and their Proposed Functions
Latency	Hematoma Inflammation Recruitment of mesenchymal stem cells Periosteal callus and cartilage formation	IL-1 and IL-6 are up-regulated after osteotomy, then return to baseline. BMP-2 and BMP-4 rise during the early latency phase to accelerate differentiation of precursor cells into chondrogenic/osteogenic cells. RANKL/OPG ratio increases by the late latency phase in association with cartilage resorption. BMP-6 and TGF- $\beta$ expression rise during the late latency phase, due to the role they play in endochondral ossification.
Active Distraction	The callus is stretched. Cartilage resorption and endochondral bone formation. Formation of a central fibrous interzone comprised of fibroblast cells and collagen fibers aligned parallel to the vector of elongation. Neo-angiogenesis between collagen fiber bundles. Osteoblast recruitment and arrangement along the new vessels, followed by intramembranous ossification and bone column formation.	IL-6 rises again during this phase to contribute to intramembranous ossification by enhancing the differentiation of cells committed to the osteoblastic lineage. RANKL/OPG ratio remains high during the early distraction phase to promote resorption of the remaining mineralized cartilage formed during the latency phase. BMP-6 expression remains high during the early distraction phase. BMP-2, BMP-4, and TGF- $\beta$ expression peak during this phase to stimulate uninterrupted bone formation in response to strain caused by distraction. IGF-1 and bFGF are induced during this phase. VEGF and angiopoietin-1 and -2 are up-regulated to stimulate new vessel formation and enhance the plasticity of existent larger vessels.
Consolidation	Bone columns interconnect. Osteoclast recruitment. Remodeling.	BMP-2, BMP-4, and bFGF expression gradually disappears. TNF- $\alpha$ markedly increases toward the end of the consolidation phase, suggesting that it regulates bone remodeling.

**Figure 3: Distraction Osteogenesis Stages and Their Biological Processes.** Figure taken from Ai-Aql et al., 2008.

### ***Bone Morphogenetic Proteins***

Bone Morphogenetic Proteins belongs to a superfamily of proteins called Transforming Growth Factor Beta (TGF $\beta$ ) (Ai-Aql et al., 2008; Bragdon et al., 2011). A group of proteins from the BMP family were identified as the primary signaling molecule for bone regeneration. BMPs elicit their biological effects by binding to type I and type II serine/threonine kinase receptors which then activate the Smads pathway (Bragdon et al., 2011). BMPs can also express their function by activating Smads-independent pathways (Bragdon et al., 2011). A multitude of cells related to maintaining the bone's environment produce BMPs such as hypertrophic chondrocytes, osteoblasts, and smooth muscle cells (Bragdon et al., 2011).

Bone Morphogenetic Protein 2 (BMP2) is well established in the literature as a growth factor responsible for bone repair (Bragdon et al., 2011; Jain, Pundir, & Sharma, 2013; Lissenberg-Thunnissen, De Gorter, Sier, & Schipper, 2011; Matsubara et al., 2012). Osteoblasts produce BMP2 and depending on which cell the BMP2 binds to, it initiates chondrogenesis and osteogenesis. (Jain et al., 2013; Lissenberg-Thunnissen et al., 2011). If BMP2 binds to osteoprogenitors, it will cause differentiation to promote osteogenesis (Ogasawara et al., 2004). When BMP2 stimulates chondrocytes, it promotes chondrocytes to proliferate and maturation (Shu et al., 2011). Moreover, BMP2's effects range from embryonic development of the heart to skeletal repair throughout life (Bragdon et al., 2011).

### ***Angiogenesis***

It is known that bone repair requires angiogenesis, the process that involves growth of new blood vessels (Kusumbe et al., 2014; Matsubara et al., 2012). There are two main types of angiogenesis: sprouting angiogenesis and intussusceptive angiogenesis, also known as splitting angiogenesis. The difference between sprouting and intussusceptive vessel formation is that the former involves *de novo* vessel formation and the later refers to new vessel elements by splitting mature vessels by inserting new extracellular matrix in the lumen of the vessel. However, it is only sprouting angiogenesis that has been associated with bone formation (Lu et al., 2006; Percival & Richtsmeier, 2013). In this study, we focused on sprouting angiogenesis as there are no known markers

for intussusceptive angiogenesis even though angiopoietin 1 and 2 have been suggested to be identifiers for intussusceptive angiogenesis (Burri et al., 2004).

The steps for sprouting angiogenesis involve degradation of capillary's basement membrane followed by endothelial cell proliferation. The endothelial cells that direct angiogenesis are selected by the proximity the cell to the highest concentration of VegfA (Gerhardt, 2008). These cells, known as the tip cells, migrate towards the source of VegfA and the trail left behind is filled by proliferating endothelial cells. When the tissue is fully perfused the vessels are then stabilized by pericytes, a type of smooth muscle cell which contain smooth muscle actin, and the basement membrane is reformed. The pericytes lie within the basement membrane of the vessels beneath the endothelial cell (Otrock et al., 2007).

Angiogenesis allows the fracture site to be fully nourished and presents signaling molecules through the vasculature that both support the progression of bone repair and then subsequent bone remodeling. (Matsubara et al., 2012). Recently, it was discovered that BMP2 is expressed by both smooth muscle cells and endothelia cells in vessels (Matsubara et al., 2012). This leads to questions as to the role that BMP2 plays in the new vessel formation during bone repair or in the tissues that are fed by these newly formed vessels during bone repair. Therefore, we crossed a tamoxifen inducible smooth muscle actin (SMA) Cre mouse with a BMP2 floxed mouse in order to conditionally delete the BMP2 gene in SMA positive cells. Several known angiogenesis markers are identified such as vascular endothelial-cadherin (ve-cadherin), vascular endothelial growth factor A (VegfA), vascular endothelial growth factor receptor 2 (VEGFR2), endomucin, and

platelet endothelial cell adhesion molecule (Pecam1) to track the development of new vessels.

Ve-cadherin, also known as Cdh5, is a cadherin molecule displayed by endothelial cells (Adams & Alitalo, 2007). Cadherins molecules allow endothelial cells to tightly bind to each other to create an impermeable barrier to allow the endothelial cells to regulate molecular transport across the lumen (Venkiteswaran et al., 2002). VEGFR2, also known as KDR, is a receptor for the VegfA molecule which is the strongest growth factor to stimulate angiogenesis (Otrock et al., 2007). Endomucin is another marker for angiogenesis as it is involved with focal adhesion assembly of endothelial cells (Ueno et al., 2001). Also, endomucin is known to be associated in bone formation as indicated by its presence in vessels formed during osteogenesis (Kusumbe et al., 2014). Pecam1, also known as CD31, is prominently used for immunohistological labelling for endothelial cells which are important cells involved in vessel formation (Parums et al., 1990).

### ***Cre-loxP System***

Due to embryonic lethality when using traditional genetic knockout of BMP2, we used a genetic strategy that bypasses this problem by using the Cre-loxP system (Bragdon et al., 2011; Haruyama, Cho, & Kulkarni, 2010). Cyclization recombinase (Cre), a 38 kDa monomeric protein, is encoded by bacteriophage P1 (Ghosh & Duyne, 2002). The tyrosine recombinase identifies, binds, and cleaves to the locus-X-over P1 (*loxP*) site which consists of a specific set of 34 base pair of DNA as shown in Figure 4. (Ghosh & Duyne, 2002; Pechisler, 2004).

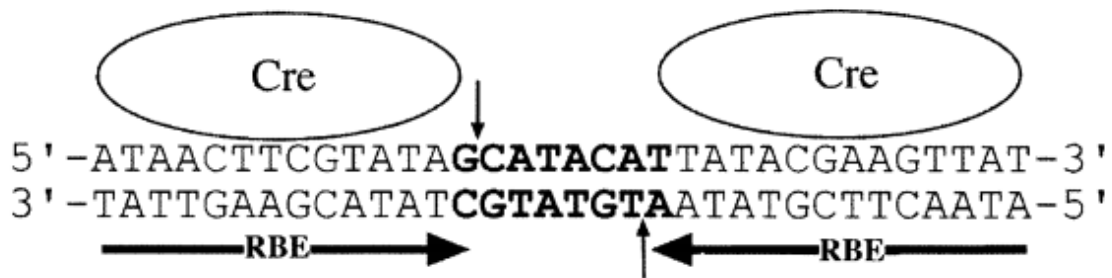


**Figure 4:** Cre-lox system. The Cre binds to the recombinase binding element (RBE) located at the *loxP* site. The vertical arrows indicate where the Cre recombinase will cleave. Figure taken from Ghosh & Duyne, 2002.

A tissue specific promoter can be implemented in mammalian models for conditional control of the *Cre-loxP* system (Kyrkanides, Miller, Bowers, & Federoff, 2003). When activated, the *Cre-loxP* system conditionally deletes the gene that is flanked by the *loxP* site in the specific cell types that are expressing the promoter driving the expression of Cre recombinase as shown in Figure 5. This molecular tool allows this study to investigate how the conditional deletion of BMP2 in smooth muscle actin expressing cells affects osteogenesis and angiogenesis *in vivo*.

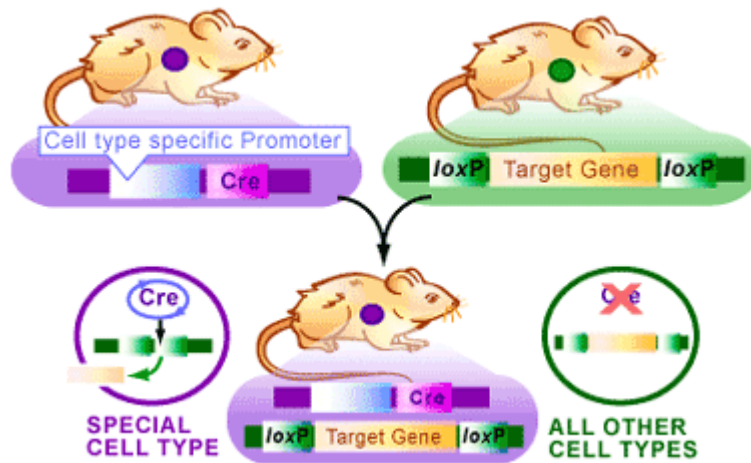


**Figure 5: Tissue-specific *Cre-loxP* system.** How the *Cre/loxP* system can be tissue/cell type specific by adding specific promoters. For our study, the cell type specific promoter is smooth muscle actin positive cells and it is inducible by tamoxifen. The target gene is the BMP2. When the two mice are crossed, it will create a strain of transgenic mouse containing SMA Cre x BMP2 flox. The Figure taken from Pechisker, 2004.



In our studies we used a smooth muscle actin promoter to conditionally target the recombination of BMP2 in primarily vascular smooth muscle cells. In these studies the SMA promoter was further temporally regulated by the addition of a tamoxifen inducible element that allowed us to only drive Cre from the SMA promoter after the induction by the addition of tamoxifen.

### ***Experimental Aims***

It is known that angiogenesis is required for proper bone healing and bone regeneration however the relationship between vessels and bone is not completely understood. Since BMP2 is known to be expressed in vessels by multiple cell types during DO, it is possible that BMP2 that is produced by these cells contributes to this link. This study will identify relationships and roles of BMP2 signaling for angiogenesis and osteogenesis during DO. This is clinically relevant as knowledge of how BMP2 operates can be used in the medical field in a precise way to modulate healing process. To investigate, we deployed an experimental timeline as shown in Figure 6 which includes distraction osteogenesis in conjunction with tamoxifen-induced BMP2 deletion in SMA expressing cells.

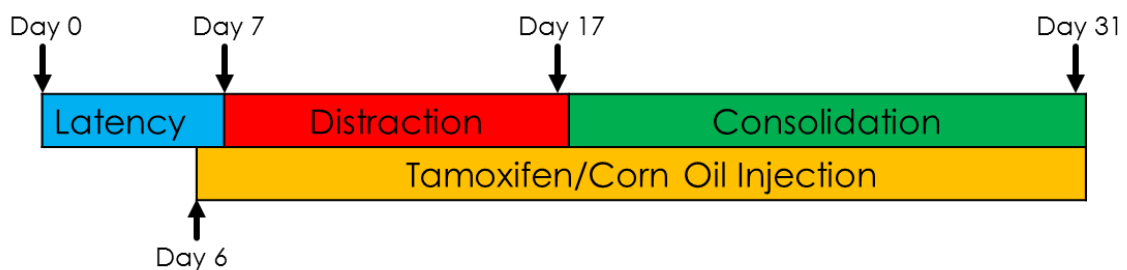


**Figure 6: Experimental Timeline.** Experimental timeline where the blue box represents a latency period, red box represents the distraction period, green box represents a consolidation period, and yellow box represents the tamoxifen-

induced BMP2 knockout phase. The top arrows indicate specific time points where we obtained x-ray, RNA, and  $\mu$ CT results. The day 6 arrow indicates beginning of tamoxifen or sterile corn oil injections.

The gene expression profiles for skeletal repair and angiogenesis will be collected for both femur and muscle that have known functions in skeletal repair and angiogenesis. Furthermore, X-ray images,  $\mu$ CT bone evaluation and  $\mu$ CT vessel perfusion scans will be conducted to gain an overall picture of how angiogenesis affects osteogenesis.

## MATERIALS AND METHODS

### *Animal Model*

All animals used in this study met the requirements of an approved IACUC protocol which complies with all federal and USDA guidelines. The transgenic mouse model used for this study was originally from Dr. Steve Harris (Yang et al., 2012). All the mice used in the study were 13 to 15 weeks old male mice at the time of the surgical procedure. The transgenic strains of mice used are SMA Cre/BMP2 Flox; Rosa dTomato x SMA Cre BMP2 Flox; and LacZ Rosa x SMA BMP2 Flox. A total of 104 male mice were used for this study. Shown below in Table 1 are the time points and the number of samples per time point and their purpose.

Time point	Number of Samples	Purpose
Day 0	3	qPCR
Day 3	3	qPCR
Day 7	4	qPCR
Day 12	11	qPCR
Day 17	12	qPCR
	17	Bone evaluation
	10	Vessel perfusion
	5	Histology
Day 24	6	qPCR
	4	Bone evaluation

	1	Histology
Day 31	7	qPCR
	13	Bone evaluation
	8	Vessel perfusion
	1	Histology

**Table 1: Enrollment of animals and their uses.**

### ***List of Common Reagents Used***

Common reagents and equipment used for this study are listed below in Table 2.

<b>Reagents</b>	<b>Manufacturer</b>
Phosphate buffered saline (PBS), Taqman Reverse Transcription Kit, Universal Master Mix, and Appropriate Primers	Applied Biosystems™
Enrofloxacin	Baytril®
Povidone-iodine	Betadine®
Buprenorphine	Buprenex®
Barium sulfate (Catalog No: 764)	E-Z-EM Canada Inc.
Curing agent for MicroFil and MicroFil	Flow Tech, Inc. Carver, MA
10% Phosphate buffered formalin, NaOH pellets, TAE buffer	Fisher Scientific™
Isoflurane	Henry Schein®
Agarose, Chloroform, Ethanol, Ethylenediaminetetraacetic acid (EDTA),	Sigma-Aldrich®

Gelatin, Hydrochloric Acid (HCl), Isopropanol, Paraformaldehyde (PFA), and Tamoxifen	
--	--

**Table 2: Common reagents and equipment used for the study.** Listed in this table are reagents and equipment regularly used for the study along with their respective manufacturer. The table is organized in alphabetical order with respect to the reagents and equipment.

### *Surgical Procedure for Distraction Osteogenesis*

Surgical procedures were performed in a chemical fume hood and was maintained with a non-fenestrated sterile field (Busse Inc.) and absorbant bench underpad (VWR<sup>®</sup>). Mice were anesthetized with 4% isoflurane /oxygen mixture using the Isotec 3 machine (Ohmeda<sup>®</sup>). Once unresponsive to physical stimuli, mice were maintained at 2% isoflurane/oxygen mixture and heat was provided with a heating pad to maintain homeostasis.

Mice received pre-operative analgesia (0.1mL buprenorphine) and antibiotic (0.01mL of enrofloxacin). The left limb was shaved and cleaned using povidone-iodine. An incision of one inch was made parallel to the femur from the greater trochanter to the knee (Lybrand, Bragdon, & Gerstenfeld, 2015). The femur was exposed by opening the muscle fascia layer posterior and anterior to the femur (Lybrand et al., 2015). The distraction device was opened to an approximate length of 3.0mm. The distraction device was then attached to the femur using 0.012 inch thin stainless steel wires (Standard Kobayashi Hooks) threaded at the greater trochanter and another wire posterior to the femur at the knee (Lybrand et al., 2015). A second set of wires were used to secure the distraction device in place using the same process. Once the distraction device was

securely fastened, a tissue elevator was positioned to protect the surrounding muscle tissue and a transverse osteotomy was created using a hand grinder (Model: Gx-7, A.M.D. Dental Mfg., Inc.) with a circular saw attachment (Brasseler USA<sup>®</sup> Lot No. J4271). The fascia was sutured using C-3 6-0 surgical plain gut suture (Hu-Friedy<sup>®</sup>) and the skin was sutured closed using absorbable C-1 5-0 surgical plain gut suture (Hu-Friedy<sup>®</sup>).

Using an animal scale (Adam Equipment<sup>®</sup>), post-surgery weight was recorded. Mice were monitored for 20 minutes to observe the animal was walking correctly. Post-operative care was provided for 48 hours post-surgery. Mice received 0.10mL of buprenorphine and 0.01mL of enrofloxacin.

### ***Distraction Procedure***

Distraction phase started at day 7 and continued for 10 days. A distraction tool was used with the distraction device producing a quarter turn twice daily (0.15 mm/day) until the target date. The total length of distraction was 1.5mm.

### ***Control Injections***

The corn oil was sterile filtered using a 0.22µm filter unit (Millex<sup>®</sup>GP) and 10mL syringe (BD<sup>®</sup>) and aliquoted into sterile 1.8mL cryotubes (Model: Nunc<sup>®</sup>, Sigma-Aldrich). The corn oil was stored in a -20°C freezer to ensure sterile conditions. Controls received IP injections of sterile corn oil starting at day 6 and continued throughout the experiment (3x per week).

### ***Tamoxifen Injections***

Tamoxifen was dissolved in corn oil at a concentration of 10mg/mL in a 50mL conical tube by using a sonicator. Each sonication cycle consisted of 30 seconds on and 5 seconds off. Sonication continued until the tamoxifen was fully dissolved in the corn oil. The solution was then sterile filtered using a 0.22µm filter unit (Millex®GP) and 10mL syringe (BD®). Tamoxifen dissolved in corn oil were aliquots of into sterile 1.8mL cryotubes (Model: Nunc®, Sigma-Aldrich) and stored in -80°C freezer to ensure sterile solutions at injections.

Mice received tamoxifen by IP injection starting at day 6 and continued throughout the experiment (3x per week). Tamoxifen, at 10mg/mL in corn oil, was injected at 1% v/w of the mouse.

### ***Harvest Procedure***

Mice were euthanized using carbon dioxide followed by cervical dislocation. Plain film X-rays of the distracted limb were collected using the Faxitron® MX-20 Specimen Radiography System. Images were collected at 30kV for 40 seconds at a distance of 15 cm. After X-ray, the sample was collected by isolating the femur and removing the distraction device. The contralateral femur was also collected. For RNA samples, the superficial muscle was removed and only the distraction gap was kept from the femur as the femoral heads were removed. Muscle samples were taken from the muscle that was adjacent to the femur. All samples for RNA analysis were flash frozen in

liquid nitrogen and stored at -80°C. For vessel perfusion samples, the femur and surrounding muscle were kept intact.

### ***RNA Extraction***

For these studies a Qiagen Tissue Lyser II system was used for rapid tissue lysis and RNA extraction. Cold adaptors were used throughout lysing procedure to prevent any RNA degradation. Samples of femur or muscle were added to sterile 2mL Eppendorf tube filled with 0.75mL of Qiazol Lysis Reagent. Samples were then snap frozen by placing each tube in liquid nitrogen for 10 to 20 seconds to allow the stainless steel bead to pulverize the sample in its solid form. Tubes were quickly placed into the Qiagen Tissue Lyser II sample holders, added one stainless steel bead, and capped the holders with its adaptors. The Qiagen Tissue Lyser II ran for 2 minutes at a frequency of 30 Hz for each cycle. If the bone is not fully ground, the cycle is repeated again. If the sample started to thaw, it was taken out of the holder, snap frozen for 10 seconds, and lysed until the frozen solid turns into a whitish pink solution.

Each sample was transferred into a new autoclaved 2mL filled with 1.0mL of Qiazol Lysis Reagent, and placed on ice for a minimum of 2 minutes to allow the lysis reagent to allow further lysing of tissue. Then 200µL of chloroform was added to the solution, thoroughly vortexed and placed on ice for 2 minutes. The solution was vortexed again and placed it in the 5804R centrifuge (Eppendorf®) at 14,000 rpm at 4°C for 15 minutes to separate the aqueous and organic layers.



The aqueous phase was transferred to another autoclaved 2mL tube then added an equal volume of isopropanol. The tube was gently inverted until the solution is clear to allow nucleic acid and other salts to fully dissociate into the solution. The solution was centrifuged in the 5804R centrifuge (Eppendorf®) at 14,000 rpm at 4°C for 30 minutes to generate a pellet.

Afterwards, the supernatant was discarded and 500µL of 70% ethanol was aliquoted to the tube to wash the RNA. The samples were then spun at 14,000 rpm at 4°C for 5 minutes in the 5804R centrifuge. An additional wash step involving 70% ethanol was used to ensure the RNA sample was free of impurities. Samples were then dried for 30 minutes by leaving the tubes upside down on a kimwipe (Kimberly-Clark®) with the lid opened. The pellet was then resuspended in 30 to 100µL of RNase-free H<sub>2</sub>O depending on the size of the pellet.

To analyze the quantity and quality of the RNA, the DU® 530 Life Science UV/Vis spectrometer (Beckman Coulter™) was used. The program used was the 260/280 assay program under the Nucleic Acid category. After blanking the spectrometer with 100µL of dH<sub>2</sub>O, a solution of 1µL of RNA from each sample in 99µL of dH<sub>2</sub>O was placed in the cuvette to determine the  $\lambda_{260}$  value and  $\lambda_{260}/\lambda_{280}$  ratio. The  $\lambda_{260}$  value indicated the concentration of RNA (µg/µL) of the sample. The  $\lambda_{260}/\lambda_{280}$  ratio designated the quality of the RNA.

Furthermore, to ensure that the RNA samples were not degraded, the samples underwent gel electrophoresis. A 1.5% agarose gel, made from 100mL of 1X TAE buffer, 1.5g of agarose, and 10µL of GelStar™ Nucleic Acid Gel Stain (Lonza®) was

used for this procedure. The gel was casted into a gel holder in the horizontal electrophoresis chamber (Bio-Rad®). Once the gel solidified, the gel was immersed in 1X TAE buffer and each well was loaded 10 $\mu$ L of RNA solution. Each RNA solution consisted of 7 $\mu$ L of dH<sub>2</sub>O, 2 $\mu$ L of loading dye, and 1 $\mu$ L of RNA. The gel was run at 110V using the electrophoresis machine (Bio-Rad®) for 1 hour to 1 hour and 15 minutes to allow optimal separation of bands. Using a UV machine (Alpha Innotech Corporation) and ImagePro Plus software, the bands were visualized under UV light and the gel was imaged using 0.4 second to 0.6 second of exposure time depending on the brightness of the bands.

### ***cDNA Procedure***

RNA (2 $\mu$ g) was diluted with RNase-free H<sub>2</sub>O to a total volume of 10.4 $\mu$ L in a 0.2mL PCR tube (Eppendorf®). Then a master solution of reagents was added to each RNA sample which consisted of 6.61 $\mu$ L of MgCl<sub>2</sub>, 6.0 $\mu$ L of dNTP mix, 3.0 $\mu$ L of 10X Reverse Transcriptase Buffer, 1.5 $\mu$ L of Random Hexamers, 0.6 $\mu$ L of RNase Inhibitor, and 1.89 $\mu$ L of Taqman Reverse Transcriptase for a total volume of 30  $\mu$ L. The solution was thoroughly vortexed, spun down, and underwent PCR reaction using the Mastercycler personal wells (Eppendorf®). The program used for PCR was program #11 which consisted of a denaturing stage of 10 minutes at 25°C followed by an annealing stage of 60 minutes at 37°C then an elongation stage of 5 minutes at 95°C and finally the PCR machine held the solution at 4°C.

### ***Quantitative Polymerase Chain Reaction (qPCR)***

cDNA was diluted with RNase free H<sub>2</sub>O to a ratio of 1:50 with the total volume of 500 $\mu$ L. Using the repeater pipette (Eppendorf<sup>®</sup>) with a 5mL syringe (BrandTech), 10 $\mu$ L of Universal Master Mix and 1 $\mu$ L of the appropriate primer were placed into each well of the 96 well PCR plate (USA Scientific<sup>®</sup>). 9 $\mu$ L of the 1:50 diluted cDNA were added into each well using the multi-channel pipettor (BrandTech). The PCR plate was covered with clear film and centrifuged for 2 minutes at 1200 rpm. Each sample was run in duplicate.

ABI 7700 Sequence Detector<sup>®</sup> (Applied Biosystems) was used to run the qPCR reaction. The 7300 software program, used in conjunction with the ABI 7700 Sequence Detector, repeated the following cycle 40 times. Each cycle consisted of 2 minutes at 50°C then 10 minutes at 95°C followed by 15 seconds at 95°C then 1 minute at 60°C. All CT values were analyzed using the delta delta CT method which uses two normalizations, one to the control gene, 18s and two, normalizes the experimental samples to the control group (Livak & Schmittgen, 2001).

### ***Primers used for Real Time Polymerase Chain Reaction (RT-PCR)***

Listed in Table 3 are genes this study examined to describe how osteogenesis was affected by BMP2 knockout in SMA positive cells.

<b>Gene</b>	<b>Known Function/Properties</b>	<b>ID Number</b>
<b>Bone Production Genes</b>		
BMP2	Potent agonist for osteogenesis	Mm01340178_ml
ID1	Downstream of BMP2 signaling pathway; increase bone mass	Mm00775963_gl
Smad6	Involved in the Smad pathway initiated by BMP2	Mm00484738_ml
Smad7	Involved in the Smad pathway initiated by BMP2	Mm00484740_ml
Prx1	Osteoprogenitor stem cell marker	Mm00440932_ml
Osteocalcin	Binds tightly to calcium and apatite	Mm00649782_gl
Osterix	Involved in osteoblast differentiation	Mm04209856_ml
Bone Sialoprotein (BSP)	Binds tightly to hydroxyapatite	Mm00492555_ml
DMP1	Produces dentin matrix acidic phosphoprotein 1	Mm01208363_ml
SOST	Inhibitor of bone growth through inhibition of Wnt signaling	Mm00470479_ml
RUNX2	Osteoblastic differentiation	Mm00501580_ml
<b>Bone Resorption Genes</b>		
Cathepsin K	Protein involved in osteoclast function	Mm00484039_ml
Trap5b	Bone resorption marker	Mm00475698_ml
RANKL	Activating factor for osteoclast differentiation; increase bone resorption	Mm00441908_ml

<b>Chondrogenic Genes</b>		
Sox9	Part of skeletal development through association with chondrogenesis	Mm00448840_ml
Acan	Proteoglycan component of cartilage	Mm00545794_ml
Col10a	Type X collagen from hypertrophic chondrocytes	Mm00487041_ml
<b>Angiogenic Genes</b>		
Ve-cadherin	Cadherins present on endothelial cells	Mm00486938_ml
VegfA	Involved in angiogenesis, endothelial growth, and vasculogenesis	Mm00437304_ml
VEGFR2	Receptor for VegfA, VegfC, and VegfD. Involved in multiple angiogenesis activities.	Mm00440099_ml
Pecam1	Cell adhesion marker involved diapedesis during inflammation; primarily used to display presence of endothelial cells	Mm01242584_ml
Endomucin	Inhibits ability for cells to bind to extracellular matrix by inhibiting focal adhesion assembly	Mm00497495_ml

**Table 3: Genes related to bone production, bone resorption, chondrogenesis, and angiogenesis.**

### ***Micro-Computed Tomography (micro-CT) for Bone Evaluation***

Scanco Medical  $\mu$ CT 40 was used to scan the region of interest which included the distraction gap with additional space distally and proximal to the gap. Typically the scanned region was approximately 700 slices and scanned at a resolution of 9 $\mu$ m. The control file used was named, DBM\_Vessels, which dictates the proper parameters for the

scanner at the resolution of 9 $\mu$ m which are 70kV, 114 mA and 300 seconds of integration time.

In the Scanco microCT 40 analysis software, samples were contoured by drawing lines as closely to the sample as possible that included bone and surrounding callous. Any cortical bone along with the medullary cavity was excluded from the contouring to ensure that the bone evaluation only determined newly formed bone. When the 3D bone evaluations were run, the threshold used was determined by the image processing language threshold determination script, developed by Scanco Medical System. It calculated an optimal threshold for the contoured area for trabecular bone. The average threshold throughout all samples were 160. The evaluation generated a bone volume (BV) which indicated the amount of bone present per cubic centimeter and total volume (TV) which was the total contoured volume in cubic centimeters.

### ***Vessel Analysis***

Described below in the following three subsections are the methods used for investigating vessel formation involving vessel perfusion,  $\mu$ CT, and de-calification.

#### ***Vessel Perfusion***

After euthanizing the mouse with CO<sub>2</sub>, plain x-ray images were obtained with the Faxitron MX-20 Specimen Radiography System of the distracted limb using the same settings as the harvest procedure. The mouse was placed in a supine position on top of a Styrofoam platform that was angled at 30°. A vertical incision of the skin was made through the median plane starting from the abdominal cavity towards the neck followed

by two horizontal incisions that ran parallel with the bottom of the rib cage using a pair of scissors. The visceral peritoneum at the bottom of the sternum was raised by using forceps and produced a hole using scissors.

A pneumothorax was created by cutting a pin-size hole in the diaphragm using small scissors. Using the same pair of scissors, the diaphragm was separated from the rib cage and clipped the two ends of the rib cage parallel to the sternum. The ribcage was then lifted and pinned back using an 18 gauge needle (BD<sup>®</sup>) exposing the cardiac cavity. The exposed heart was used as the landmark to locate the vena cava which was snipped to create a drainage hole for the perfusion solution. The left ventricle was pierced by a 25 gauge butterfly needle (BD<sup>®</sup>), and 10mL of 10% phosphate buffered formalin solution was injected using a 10mL syringe (BD<sup>®</sup>).

Two different contrast agents were used in these studies.

### **Method 1**

In these studies, MicroFil solution was prepared using 9mL of MicroFil and 500 $\mu$ L of curing agent (Morgan et al., 2012). 6 mL of the MicroFil and curing agent mixture was injected into the mouse using 1mL TB syringes (BD<sup>®</sup>). The samples were then fixed for 3 days in PFA and washed with 1X PBS.

### **Method 2**

For the barium model, a solution was made of 6mL of Ba (25% w/v), 12mL of 1X PBS, and 12mL of gelatin/PBS (Roche et al., 2012). We made the gelatin/PBS mixture by adding 1.5g of gelatin to 50mL of 1X PBS in a 50mL conical tube. The mixture was heated in a 100°C water bath until it liquefied. The solution was allowed to cool to ~

37°C. The animals were injected with 12mL of the barium/gelatin solution to ensure consistent amount of vessel perfused between each sample. The samples were then fixed for three days in PFA and washed with 1X PBS before being embedded in agarose gel.

#### *Micro-Computed Tomography (micro-CT) for Vessel Evaluation*

Stainless steel wires (0.012 inch Standard Kobayashi Hooks) were threaded through the tissue near the proximal femoral head. Additional wires were inserted to mark the region of interest. The samples was then embedded in 2% agarose (w/v) to maintain the samples in place within the scanning tubes.

Using the Scanco Medical  $\mu$ CT 40, the region was scanned between the two pin placements which included the distraction gap. Typically the scanned region consisted of 700 slices. The control file used was DBM\_Vessels with a resolution of 9 $\mu$ m which are 70kV, 114 mA and 300 seconds of integration time. Once the scan and reconstruction completed, images were contoured by drawing a circle in the Scanco microCT 40 analysis software that included bone, vessels, and surrounding tissue. The 3D renderings were constructed using a lower threshold of 160 and a zoom of 150%. This 160 threshold was utilized because the average threshold for cortical bone to be approximately 220 and trabecular bone's average threshold was 160. The 160 threshold included vessel elements because the contrast agent used typically had a threshold greater than 160.

#### *Decalcification for Vessel Scanning*

Bones were decalcified using a 14% (w/v) EDTA solution. The tissue samples, previously embedded in agarose gel, were placed in perforated 50mL conical tubes.



Perforations were made in the tube walls by an 18 gauge needle (BD<sup>®</sup>) and further enlarged by drilling a #15 scalpel blade into it (Bard-Parker<sup>®</sup>). The tubes were immersed along with a stir bar in EDTA solution for four days on top of a stir plate (VWR<sup>®</sup>) set at 20 rpm in a 4°C room to allow total removal of mineralized tissue.

### ***Statistical Methods***

Using the JMP program, statistical analysis was performed on the qPCR Ct values using nonparametric Wilcoxon method due to the small sample size. Sample averages, standard deviation, and standard error were obtained for each group. Standard error bars were included in graphs generated for mRNA expression of selected genes.

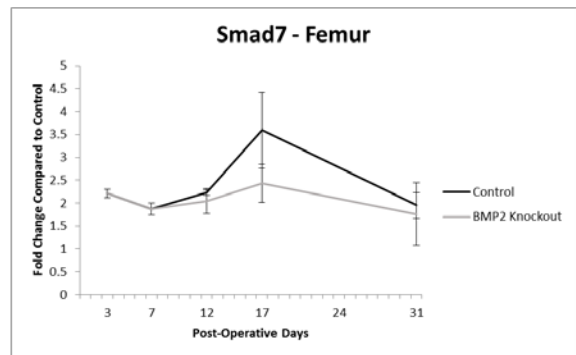
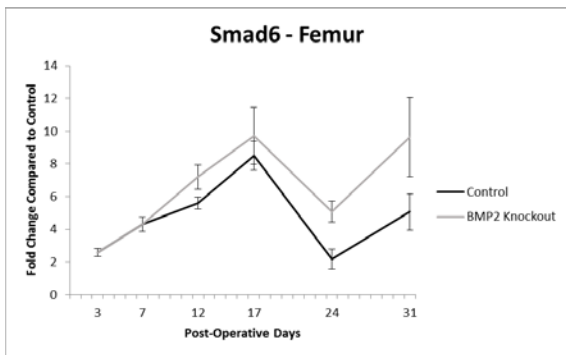
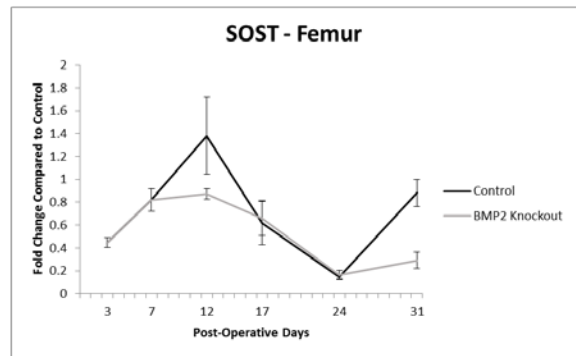
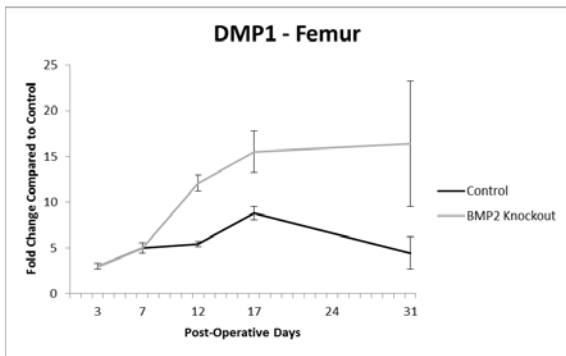
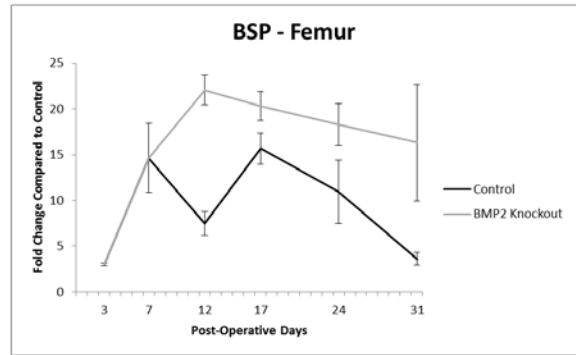
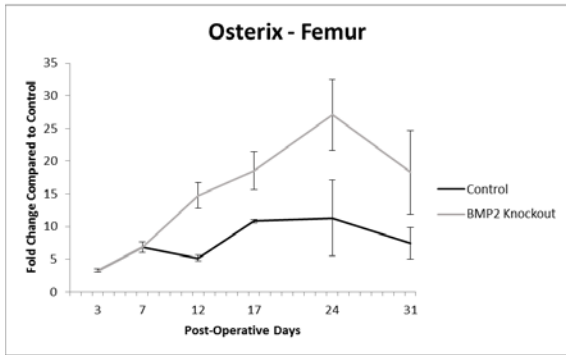
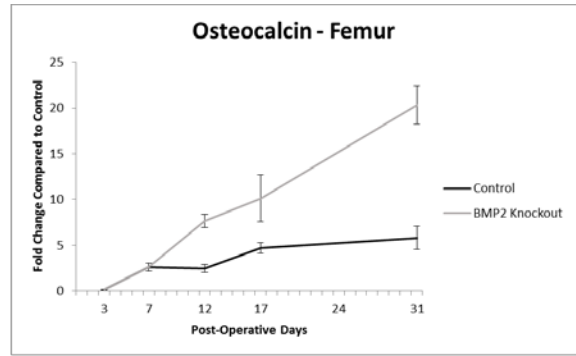
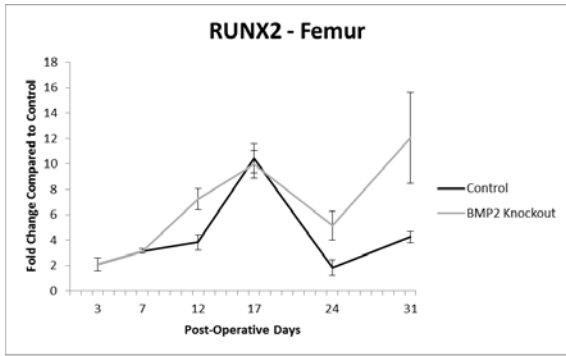
## RESULTS

### *qPCR for Distraction Gap*

RNA was isolated from samples that were collected from the distraction gap of the femur and the muscle directly adjacent to the distracted femur at days 3, 7, 12, 24, and 31. Bone formation was assessed by the analysis of a cassette of genes that defines the progression of osteogenic differentiation. In Figure 7, RUNX2 was raised for BMP2 knockout at day 12, 24 and 31 compared to the control. The control for RUNX2 had same expression values at day 17 with the knockout but dropped afterwards. Moreover, several bone production genes such as osteocalcin, osterix, BSP, DMP1, and Smad6 were increased for the BMP2 knockout compared to the control for all time points. Osteocalcin's difference between the control and knockout steadily increased from day 7 to day 31. Whereas Osterix showed increased expression between the control and knockout dipped in day 31 these results were not significantly different. Although BSP was elevated throughout all time points in the femur for the BMP2 knockout, it did not share a similar decrease in expression displayed by the control. DMP1's differences grew larger between the control and BMP2 knockout as the time points increased. There was no peak for SOST in the BMP2 knockout at day 12. SOST expression was identical between the two groups at day 17 and 24 but the BMP2 knockout showed a decreased level by day 31. BMP2 expression was higher for the knockout during the distraction phase and at the middle of the consolidation phases of the experiment. Smad6 showed similar trends between control and BMP2 knockout where the BMP2 knockout was higher in expression throughout all time points. However, Smad7 showed a different

profile in which the knockout had lower levels of expression compared to the control.

ID1 levels were elevated at all time points for the knockout. The knockout for Prx1 gene demonstrated an earlier spike in expression to the control, but increased expression at day 31.



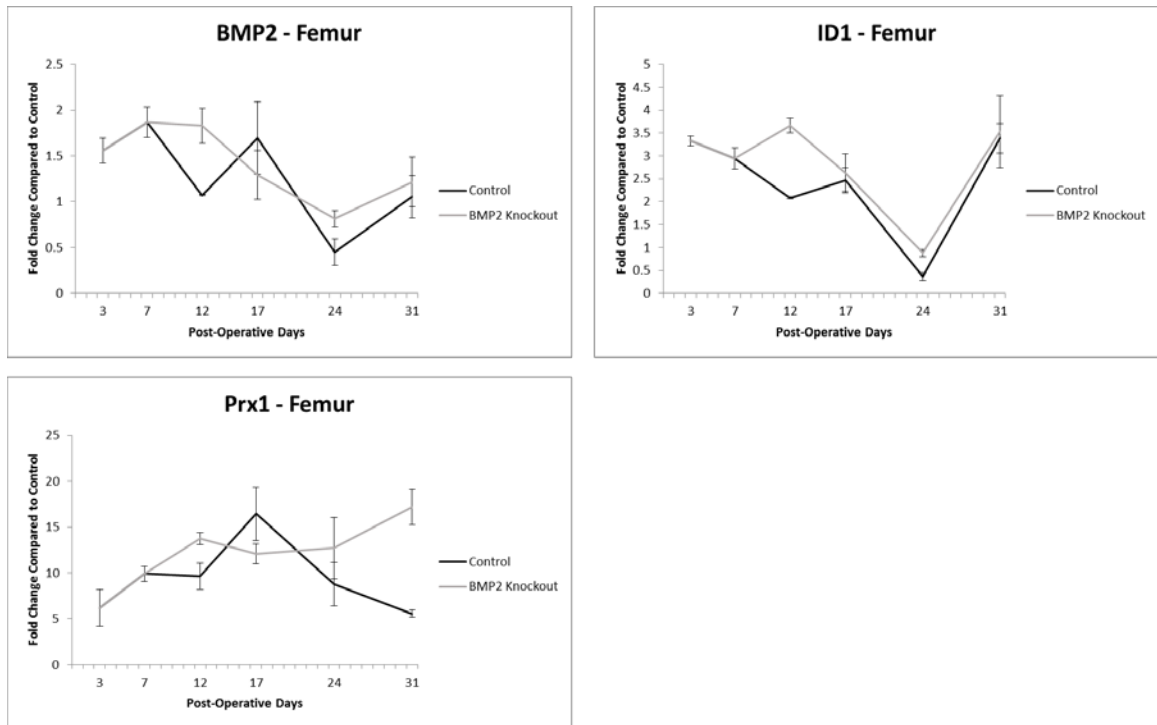


**Figure 7: Distraction Gap qPCR Results for Bone Production.** The black line represents the control (corn oil) and the grey line represents the experimental (tamoxifen-induced BMP2 knockout). RUNX2, Osteocalcin, Osterix, BSP, DMP1, SOST, Smad6, Smad7, BMP2, ID1 are bone producing factors. Prx1 is an osteoprogenitor stem cell marker. The error bars shown are standard error. There are no statistical differences ( $p > 0.05$ ) between control and BMP2 knockout for all bone producing genes. The sample size for day 3 was  $n=3$ , day 7 was  $n=3$ , day 12 was  $n=6$ , day 17 was  $n=11$ , day 24 was  $n=6$ , and day 31 was  $n=6$ .

Bone resorption genes are depicted in Figure 8. Trap5b and RANKL showed higher expression levels at day 12 for the BMP2 knockout but was quickly eclipsed by the control at day 17. The spike of the control at day 17 eventually fell below the knockout at day 31. Cathepsin K was elevated for the experimental groups compared to the control throughout all time points.

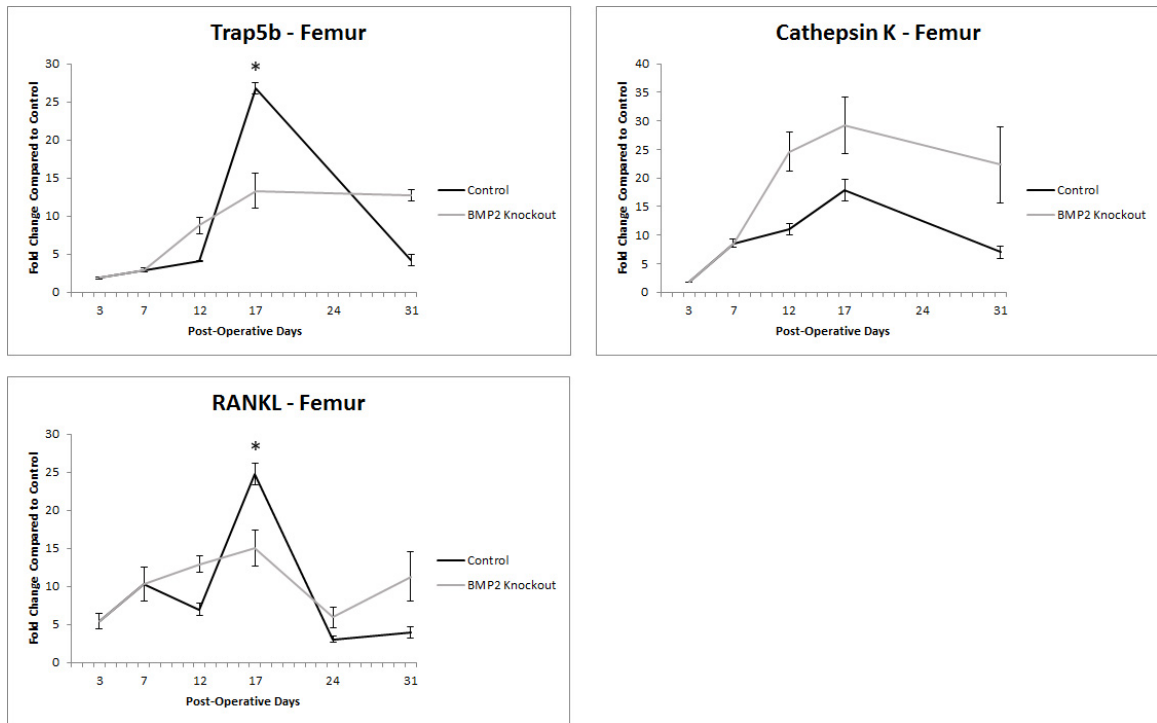


**Figure 8: Distraction Gap qPCR Results for Bone Resorption.** The black line represents the control (corn oil) and the gray line represents the experimental (tamoxifen-induced BMP2 knockout). Trap5b, Cathepsin K, and RANKL are bone resorption genes. The asterisk indicates statistical difference at that time point between the control and BMP2 knockout. At day 17, there is statistical difference for Trap5b and RANKL between the control and BMP2 Knockout with  $p < 0.05$ . The rest of the time points for Trap5b, Cathepsin K, and RANKL have no statistical difference ( $p > 0.05$ ) between the control and BMP2 knockout. The sample size for day 3 was  $n=3$ , day 7 was  $n=3$ , day 12 was  $n=6$ , day 17 was  $n=11$ , day 24 was  $n=6$ , and day 31 was  $n=6$ .

The effect of BMP2 knockout in SMA positive cells was also measured for chondrogenesis which is shown in Figure 9. Col10a profile showed a smaller and earlier peak for the BMP2 knockout than the control. The large difference in magnitude for peaks of the control to the knockout is 21577 fold, which is statistically significant. Acan, another gene for chondrogenesis, follows the same pattern as Col10a in that there was an earlier peak of expression for the BMP2 knockout samples. However, the difference in peak magnitude was not as dramatic as Col10a. Sox9 also exhibited an earlier spike in

expression but was not as pronounced as seen in Col10a and Acan. For all three genes, the expression drops after the peak.

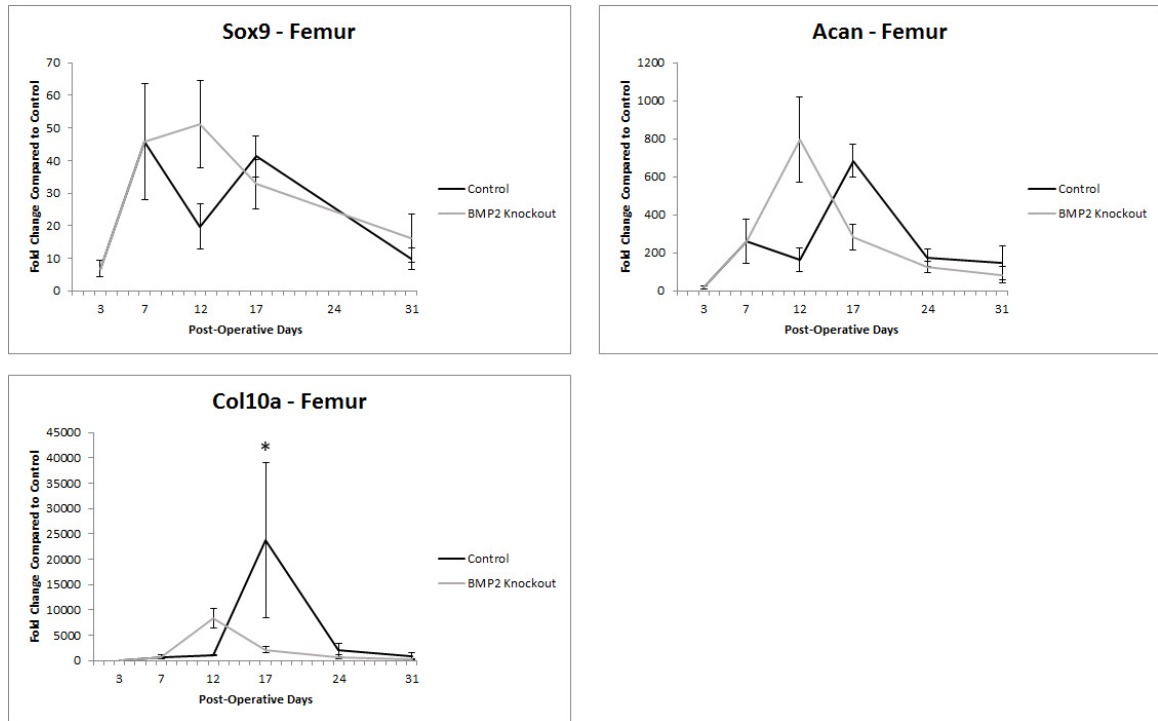


**Figure 9: Distraction Gap qPCR Results for Chondrogenesis.** The black line represents the control (corn oil) and the gray line represents the experimental (tamoxifen-induced BMP2 knockout). Sox9, Acan, Col10a are important components for chondrogenesis. The error bars shown are standard error. The asterisk indicates statistical difference at that time point between the control and BMP2 knockout. At day 17, there is statistical difference for Col10a between the control and BMP2 Knockout with  $p < 0.05$ . The rest of the time points for Sox9, Acan, and Col10a have no statistical difference ( $p > 0.05$ ) between the control and BMP2 knockout. The sample size for day 3 was  $n=3$ , day 7 was  $n=3$ , day 12 was  $n=6$ , day 17 was  $n=11$ , day 24 was  $n=6$ , and day 31 was  $n=6$ .

The effects of BMP2 knockout in SMA cells for angiogenesis in the distraction gap gene profiles are shown in Figure 10. The SMA gene profile showed that conditional knockout of BMP2 did not affect its function in the femur. There appeared to be a slight decrease in angiogenesis in the femur due to diminished levels of ve-cadherin and VEGFR2 specifically starting at day 17. However, there was no significant difference for VegfA, the main marker for angiogenesis, even at day 31 which had a 1 fold difference.

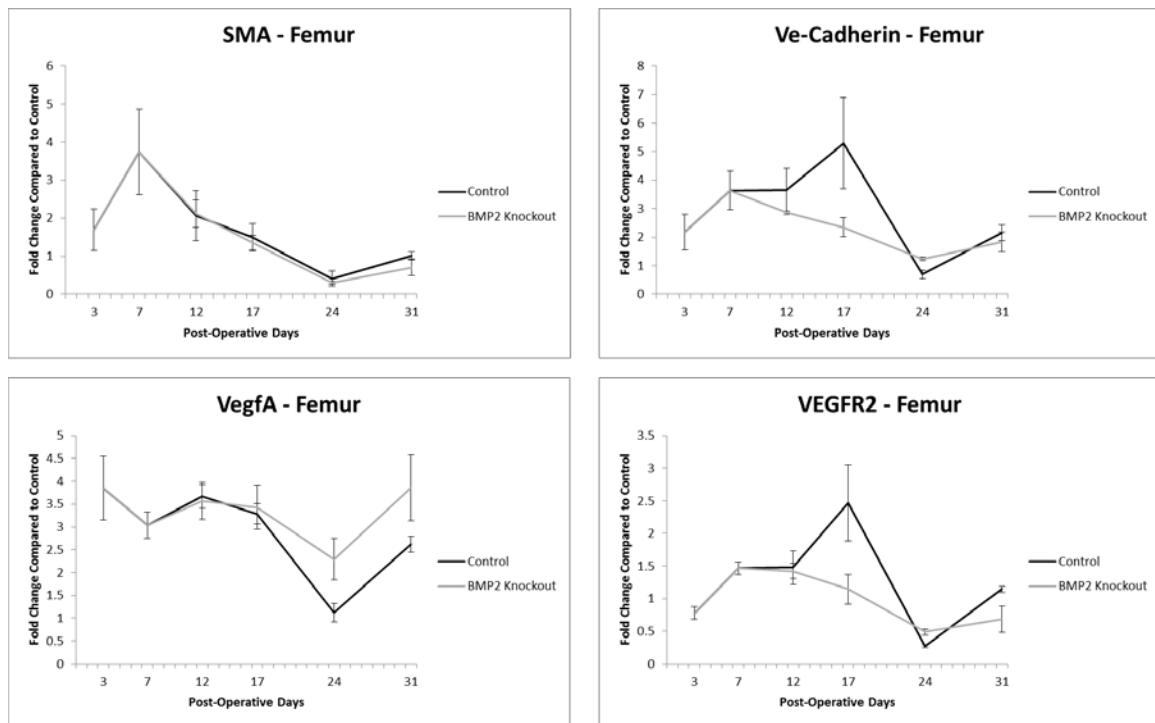
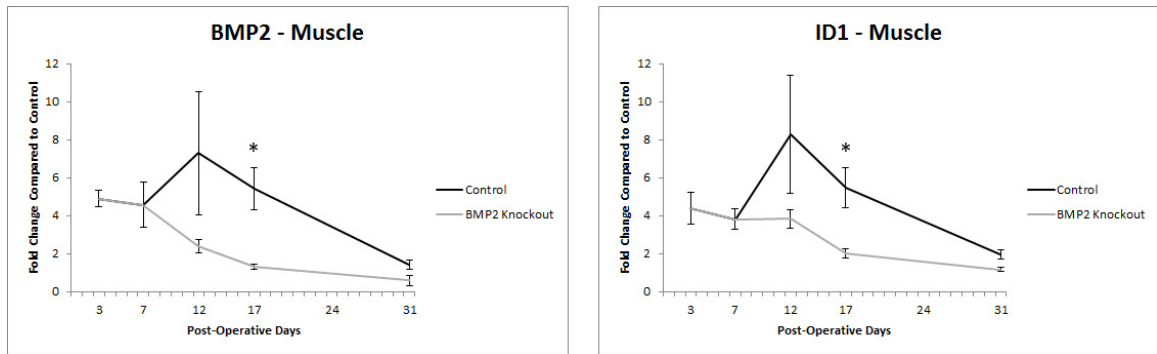


**Figure 10: Distraction Gap qPCR Results for Angiogenesis.** The black line represents the control (corn oil) and the gray line represents the experimental (tamoxifen-induced BMP2 knockout). SMA, Ve-Cadherin, VegfA, and VEGFR2 are indicative of angiogenesis. The error bars shown are standard error. All time points for SMA, Ve-Cadherin, VegfA, and VEGFR2 have no statistical difference ( $p > 0.05$ ) between the control and BMP2 knockout. The sample size for day 3 was  $n=3$ , day 7 was  $n=3$ , day 12 was  $n=6$ , day 17 was  $n=11$ , day 24 was  $n=6$ , and day 31 was  $n=6$ .

### *qPCR for Muscle*

The gene profiles of muscle for bone producing genes, BMP2 and ID1, are shown below in Figure 11. Both genes were affected by the BMP2 knockout as differences are seen as early as day 7 of the experiment with decreased expression for BMP2 and ID1. The knockout for both BMP2 and ID1 gene expressions steadily decreased towards day 31 time point. For the control, BMP2 had a small surge in expression in the muscle at day 17 whereas ID1 spikes at day 12 and then both decreased approximately linearly towards day 31.

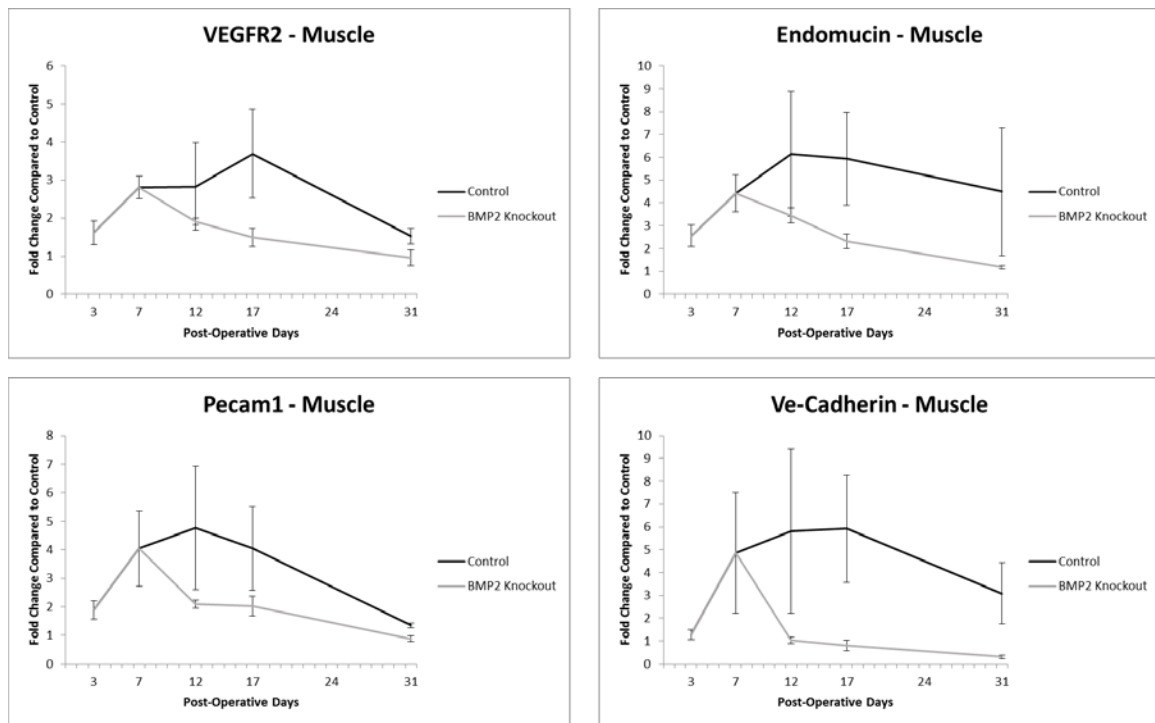




**Figure 11: Muscle qPCR Results for Osteogenesis.** The black line represents the control (corn oil) and the gray line represents the experimental (tamoxifen-induced BMP2 knockout). The error bars shown are standard error. The asterisk indicates statistical difference at that time point between the control and BMP2 knockout. At day 17, there is statistical difference for BMP2 and ID1 between the control and BMP2 Knockout with  $p < 0.05$ . The rest of the time points have no statistical difference ( $p > 0.05$ ) between the control and BMP2 knockout. The sample size for day 3 was  $n=3$ , day 7 was  $n=3$ , day 12 was  $n=6$ , day 17 was  $n=11$ , and day 31 was  $n=6$ .

Assessment of anigogenic mRNA expression in the muscle is seen in Figure 12.

A comparison of the genes expression showed every angiogenesis marker decreased 60-90% with the BMP2 knockout. The VEGFR2 profile showed decreased expression in the mice in which BMP2 was conditionally deleted in the SMA expressing cells with the largest difference at day 17 with a difference of 2 fold between the control and knockout. Interestingly, decreased levels of expression for endomucin were seen in the muscle compartment even though it had previously been selectivly associated only with vessels in the marrow space. Pecam1 levels were also decreased for the BMP2 knockout with its largest difference at day 12. This difference was reduced onwards to a difference of 1 fold at day 31. Finally an assessment of ve-cadherin expression was also shown to be reduced as well in the BMP2 knockout which suggests a diminish in angiogenesis in the muscle comaprtment. The most drastic difference occured at day 12 between the control and knockout and the difference stays relatively constant throughout the experimental timeline.



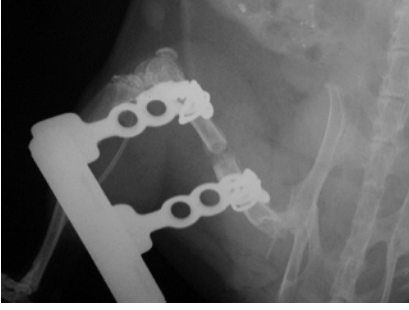







**Figure 12: Muscle qPCR Results for Angiogenesis.** The black line represents the control (corn oil) and the gray line represents the experimental (tamoxifen-induced BMP2 knockout). The error bars shown are standard error. All time points for VEGFR2, Endomucin, Pecam1, and Ve-Cadherin have no statistical difference ( $p > 0.05$ ) between the control and BMP2 knockout. The sample size for day 3 was  $n=3$ , day 7 was  $n=3$ , day 12 was  $n=6$ , day 17 was  $n=11$ , and day 31 was  $n=6$ .

## X-Ray

The development of bone during DO in control and experimental mice was initially assessed by plain X-ray film. Presented below in Figure 13 are x-ray images of the distraction device attached to the distracted femur after euthanizing the mice but before harvesting the limbs for additional BMP2 procedures. There were no significant differences in bone formed at the distraction gap between the plain X-rays for control and BMP2 knockout samples for day 7 and 17. At day 24, bone was present in the distraction gap of the control and absent in the tamoxifen induced BMP2 knockout. At day 31, the

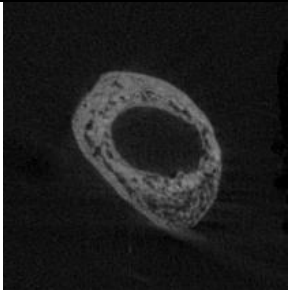
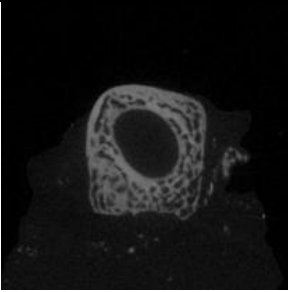
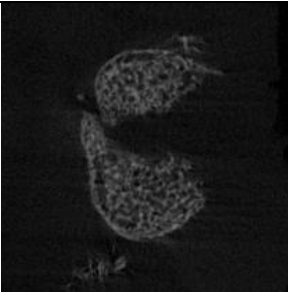
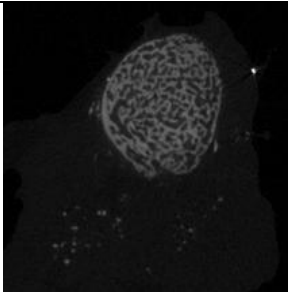
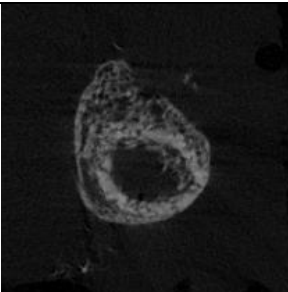
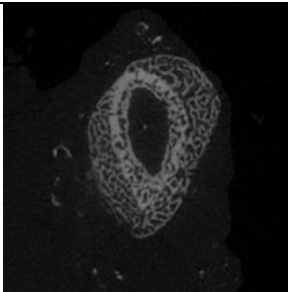
control sample's bone looked to be almost completely repaired whereas in the BMP2 knockout the distraction gap is still not filled with bone.

Post-Operative Days	Control	BMP2 Knockout
Day 7		
Day 17		
Day 24		
Day 31		

**Figure 13: DO X-ray Results.** X-ray results at different time points. The control received corn oil injections and the experimental received tamoxifen (10mg/mL) injections. These images are representative of all DO procedures.

### ***μCT Bone Evaluation***

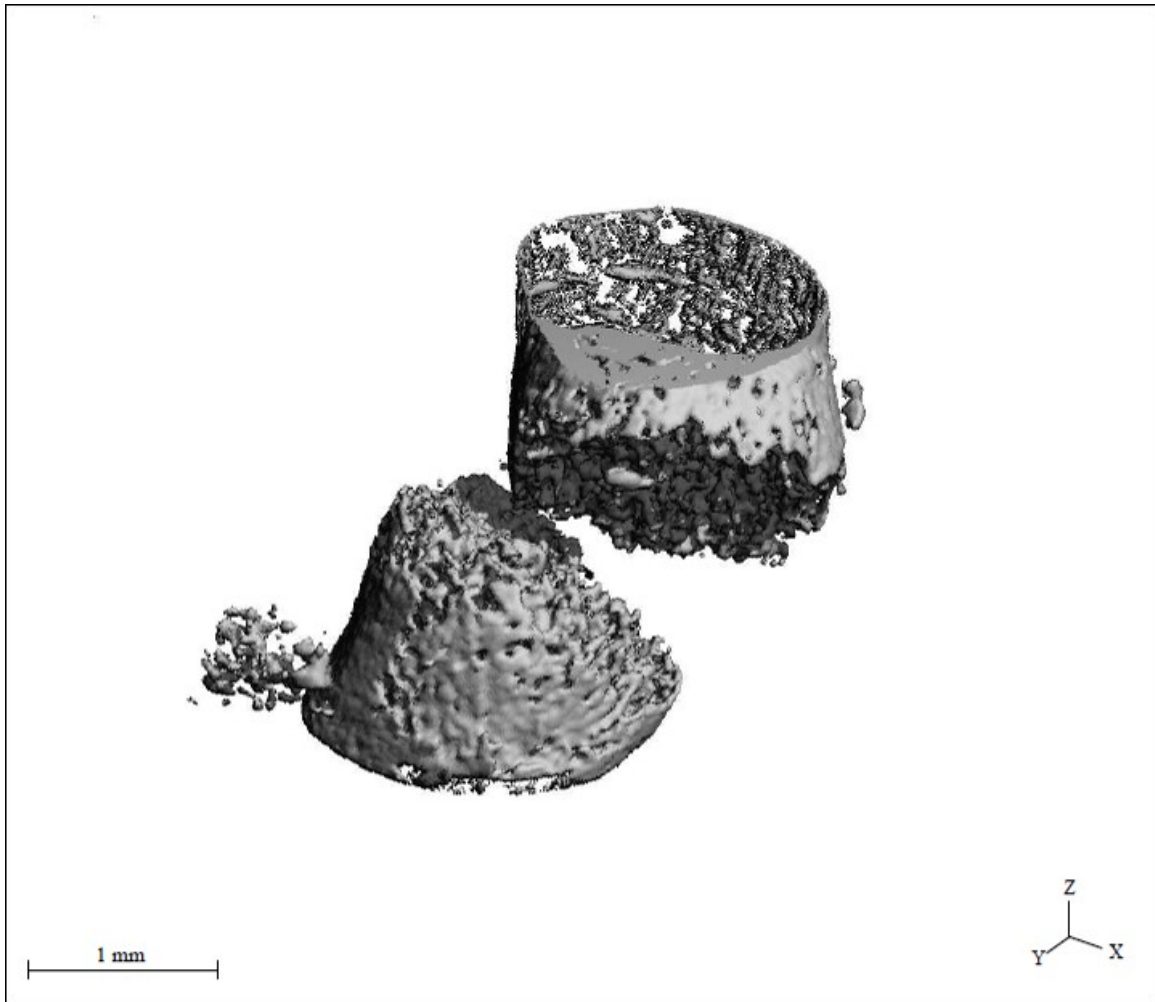
Three dimensional analysis of bone formation by μCT was completed on - samples without perfusion and were evaluated for the amount of bone present in both control and knockout samples. Shown below in Figure 14, there was no definitive difference between the knockout and the control for the two dimensional slicer viewer.

<b>Position</b>	<b>Control</b>	<b>Experimental</b>
Proximal at the region below the trochanter		
Mid-diaphyseal		
Distal to the knee		

**Figure 14: Day 31 2D μCT Results for Bone Evaluation.** Day 31 experimental μCT results of DO procedure with corn oil injections (middle column), and tamoxifen injections (far right column).

Quantitative data for bone volume (BV) for control and BMP2 knockout samples from the μCT bone scans are shown below in Figure 15 and Figure 16. The difference

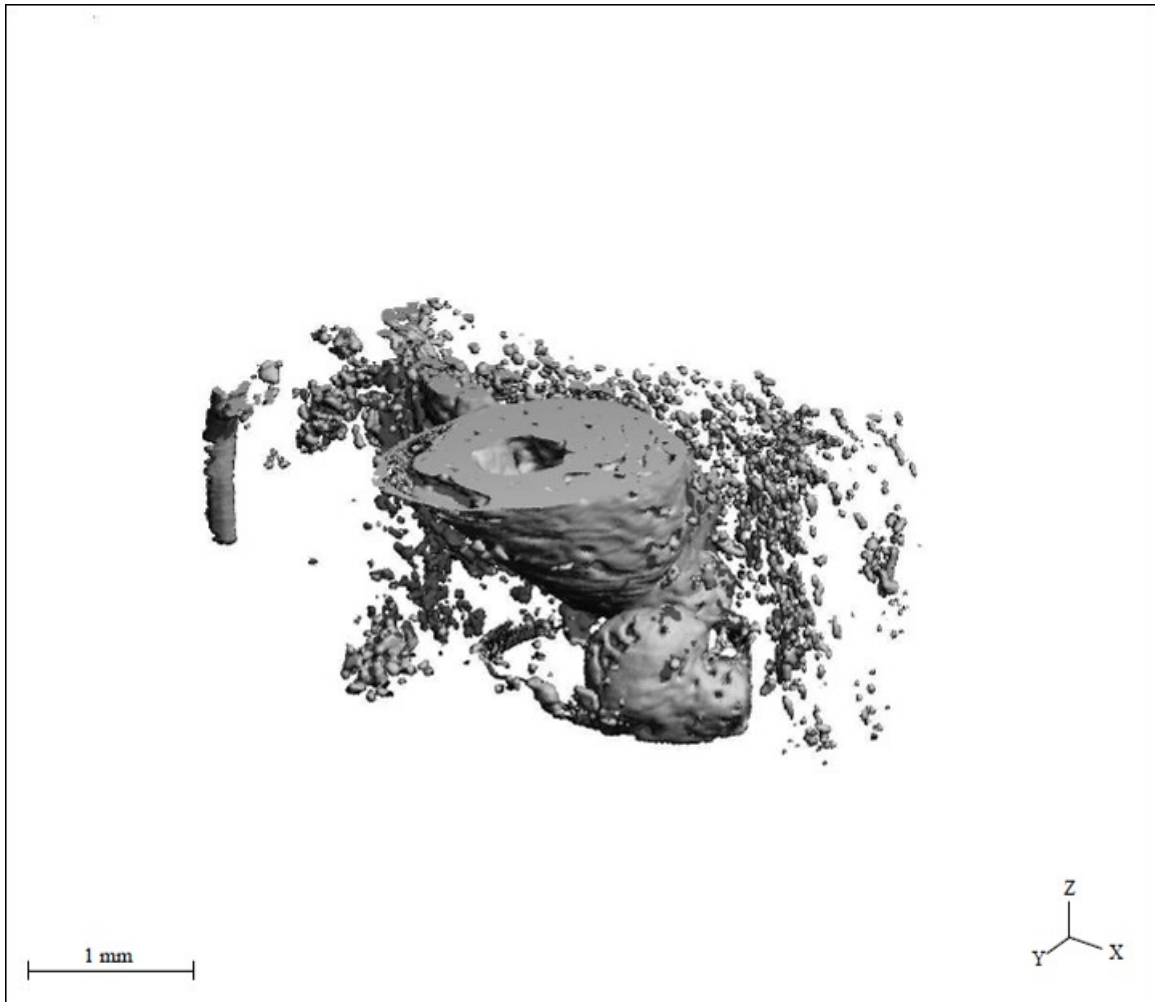
between the BV values for the control and BMP2 knockout indicated that the control had slightly more bone formed with 2.2581 mm<sup>3</sup> to knockout with 1.9492 mm<sup>3</sup> as shown in the Direct (No Model) cell. It is also shown that the control has a BV/TV value of 0.3539 which is higher than the knockout's BV/TV ratio of 0.1376.



VOI	X	Y	Z	Mean/Density [mg HA/ccm]
Position [p]	1052	882	46	of TV (Apparent) 382.9888
Dimension [p]	272	440	189	of BV (Material) 840.7435
Element Size [mm]	0.0100	0.0100	0.0100	

Direct (No Model)		TRI (Plate Model)		Anisotropy	
TV	[mm <sup>3</sup> ]	6.3809	TV [mm <sup>3</sup> ]	-	H1  [mm] -
BV	[mm <sup>3</sup> ]	2.2581	BV [mm <sup>3</sup> ]	-	H2  [mm] -
BV/TV	[1]	0.3539	BV/TV [1]	-	H3  [mm] -

**Figure 15:  $\mu$ CT Bone Evaluation for Control.** The TV, BV and BV/TV values are presented in the Direct (No Model) cell. Image is representative of all samples.



VOI	X	Y	Z	Mean/Density [mg HA/ccm]	
Position [p]	856	729	149	of TV (Apparent)	155.8379
Dimension [p]	484	372	168	of BV (Material)	869.4120
Element Size [mm]	0.0100	0.0100	0.0100		

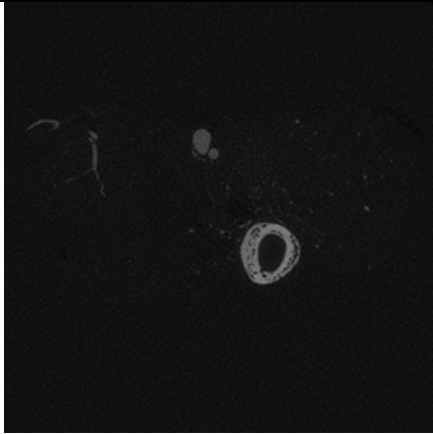
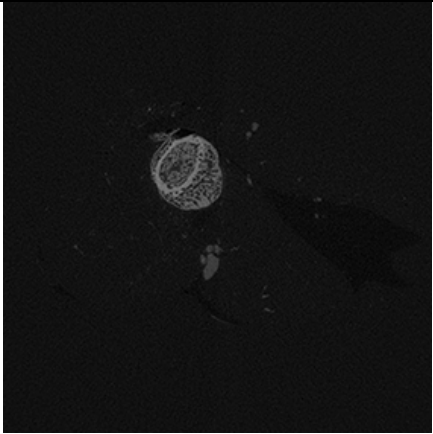
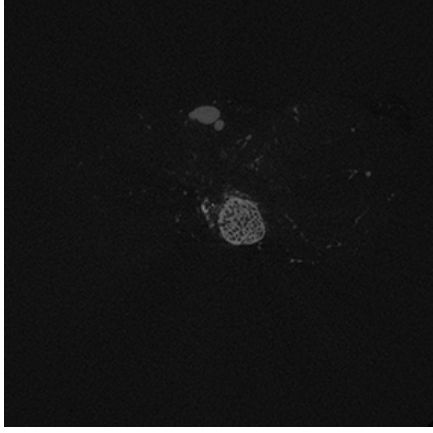
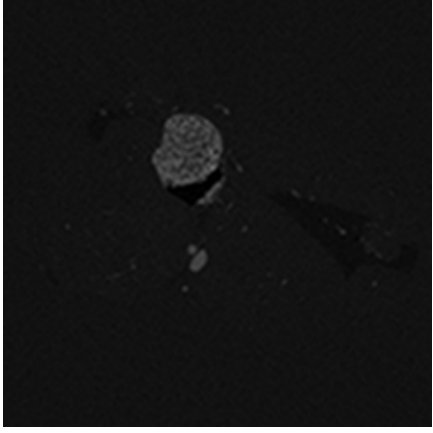
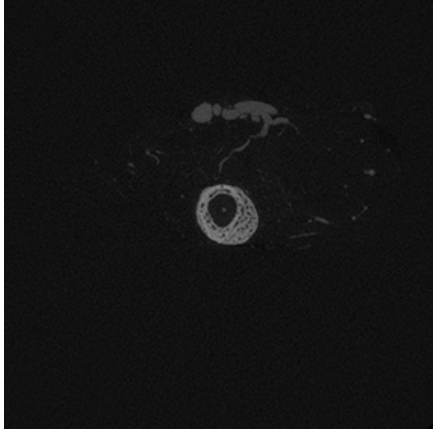
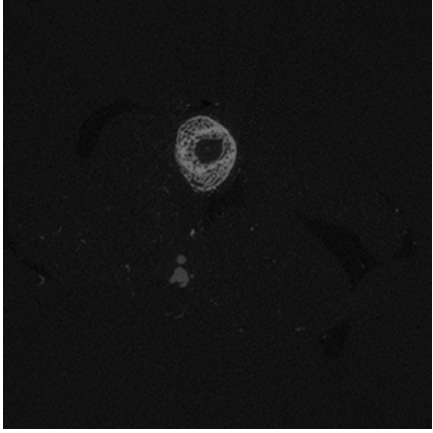
Direct (No Model)			TRI (Plate Model)			Anisotropy		
TV	[mm <sup>3</sup> ]	14.1685	TV	[mm <sup>3</sup> ]	-	H1	[mm]	-
BV	[mm <sup>3</sup> ]	1.9492	BV	[mm <sup>3</sup> ]	-	H2	[mm]	-
BV/TV	[I]	0.1376	BV/TV	[I]	-	H3	[mm]	-

**Figure 16:  $\mu$ CT Bone Evaluation for BMP2 Knockout.** The TV, BV and BV/TV values are presented in the Direct (No Model) cell. Image is representative of all samples.

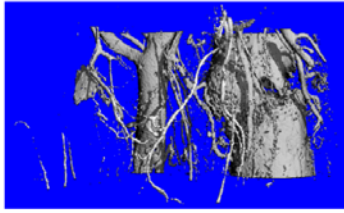
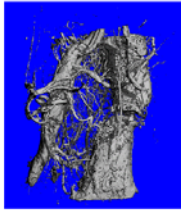
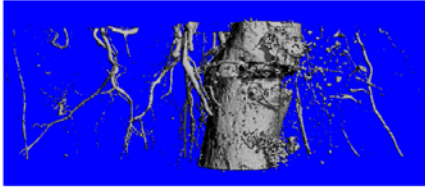
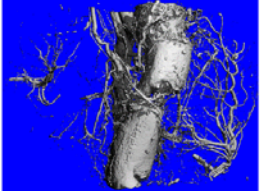
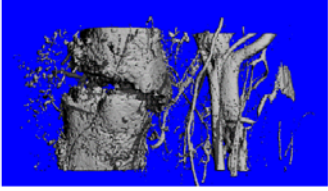
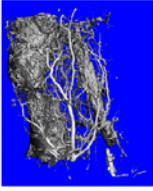


### ***μCT Microfil Vessel Perfusion***

Two dimensional slices of day 31 pre-decalcified samples for both control and tamoxifen-induced BMP2 knockout were taken as shown in Figure 17. The image sequence started at proximal at the region below the greater trochanter, mid-diaphyseal, and distal to the knee. However in the two dimensional images, it was difficult to gain a qualitative assessment of the amount of vessel present in each sample. Therefore, three dimensional renderings of pre-decalcified samples were obtained as shown below in Figure 18. These images clearly showed a difference between the control and the experimental samples in the vessels, particularly the capillaries, in which there was a smaller number of capillaries in the control compared to the tamoxifen-induced BMP2 knockout in SMA cells.

Position	Control	Experimental
Proximal at the region below the trochanter		
Mid-diaphyseal		
Distal to the knee		

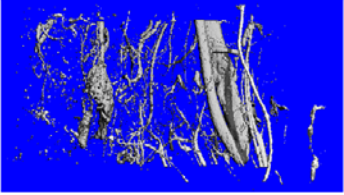
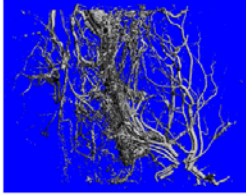
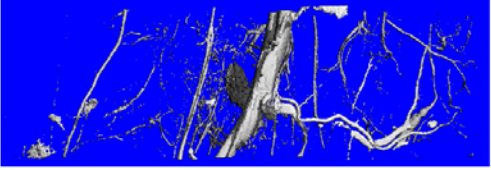
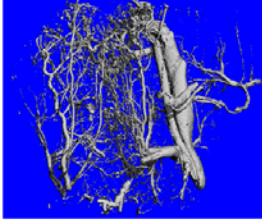
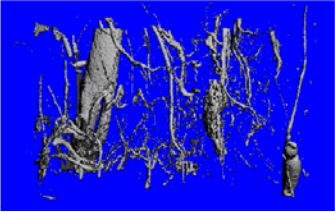
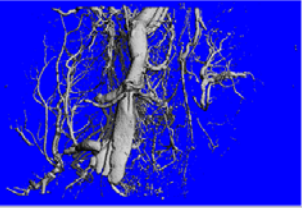
**Figure 17: Day 31 2D  $\mu$ CT Results for Vessel Perfusion.** Day 31 experimental  $\mu$ CT results of DO procedure with corn oil injections (middle column), and tamoxifen injections (far right column).

Angle	Control	Experimental
Rotation 90°		
Rotation 180°		
Rotation 270°		

**Figure 18: Day 31 3D Pre-decalcified  $\mu$ CT Results.** Day 31 experimental  $\mu$ CT results of DO procedure with corn oil injections (left images), and tamoxifen injections (right images). The rotation angle has no anatomical reference.

To further differentiate between bone and vessels, images of 3D renderings were taken after the decalcification procedure as shown in Figure 19. The decalcification procedure worked as intended as the vast majority of the amount of vessels and quality of vessels did not appear to be significantly altered. These results however were in contrast to the mRNA findings suggesting that the Microfil method may not be technically sufficient to image the smallest vessels that are present in the tissue. This conclusion was also supported by the gross appearance of the perfused tissues in the experimental groups which showed a failure to obtain complete perfusion in the distal appendages due to lack of the observed yellow color in these vessels in the BMP2 knockout experimental group. It was also noticed that in these animals often the back pressure generated by the

perfusion of the viscous Microfil reagent led to leakage of the reagent from the heart and descending aorta during perfusion.

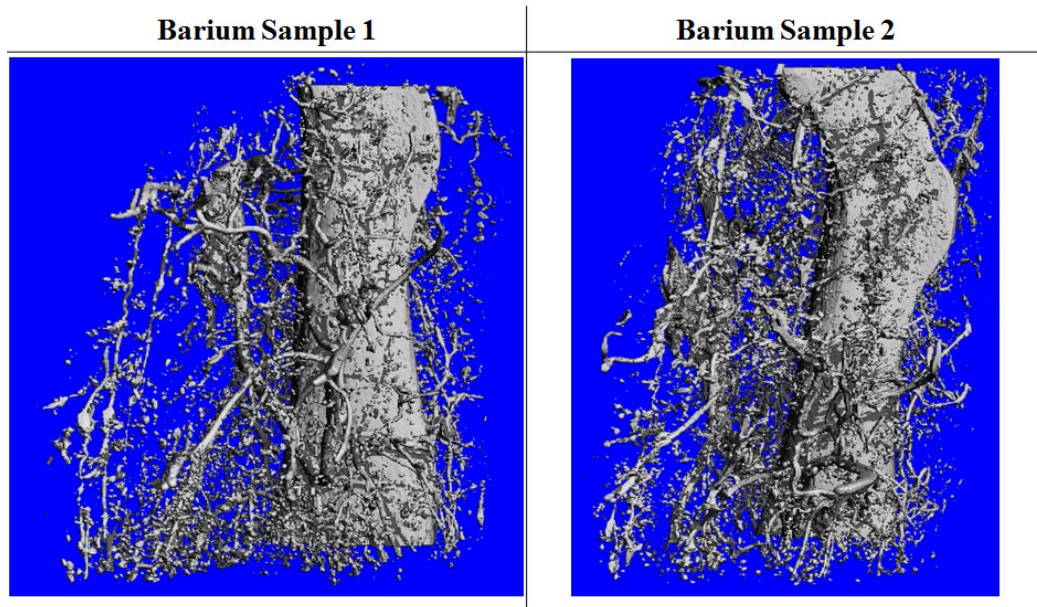
Angle	Control	Experimental
Rotation 0°		
Rotation 90°		
Rotation 180°		

**Figure 19: Day 31 3D Post-decalcified  $\mu$ CT Results.** Day 31 experimental  $\mu$ CT results of DO procedure with corn oil injections (left images), and tamoxifen injections (right images). The rotation angle has no anatomical reference.

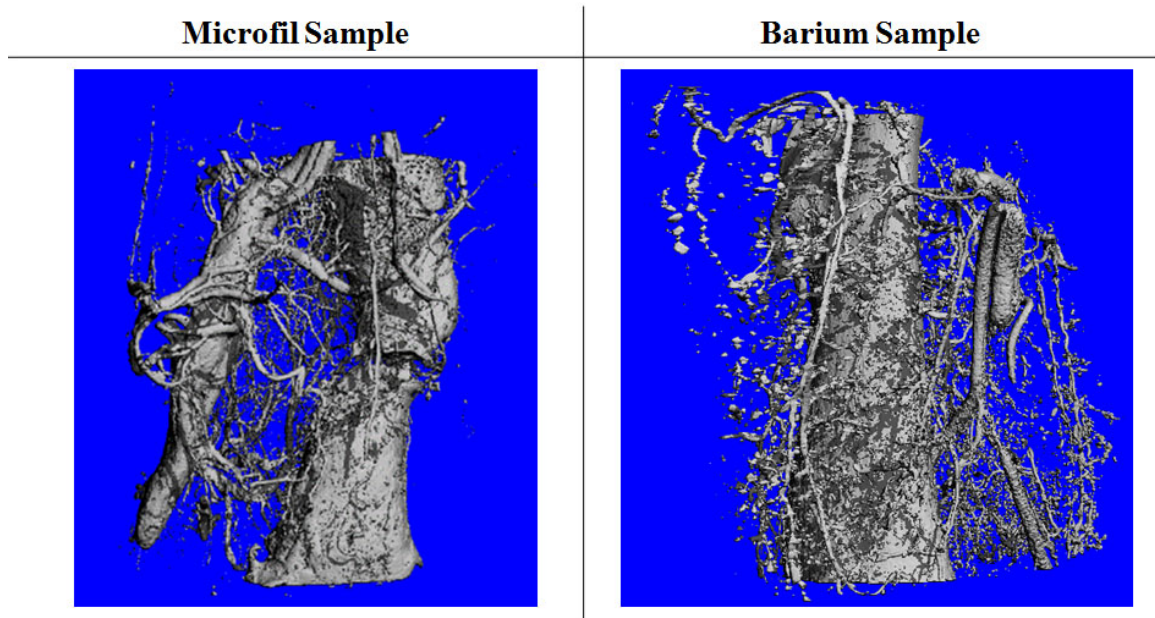
### ***$\mu$ CT Barium Vessel Perfusion***

Because of the suspected technical problems with the Microfil method, a different approach was assessed using barium solution mixed with dissolved collagen gelatin prior to polymerization. Since prior to polymerization, the gelatin solution is much less viscous than the silicon Microfil solution as well as taking much longer to set up in the vascular during perfusion this approach led to much lesser back pressure in the vasculature during perfusion as well as allows for much greater volumes of the solution to be perfused throughout the animal. The barium model results showed a much greater

reproducibility across samples and it produced a much better resolution of the smaller vessels than the Microfil method. A representative comparison of the two methods is shown in Figure 20. The two samples demonstrate the large amount of vessels perfused using 0.5g/mL of Ba in gelatin solution. Shown in Figure 21 is a comparison of barium perfused samples to Microfil perfused samples.



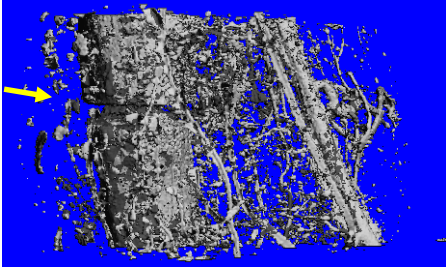
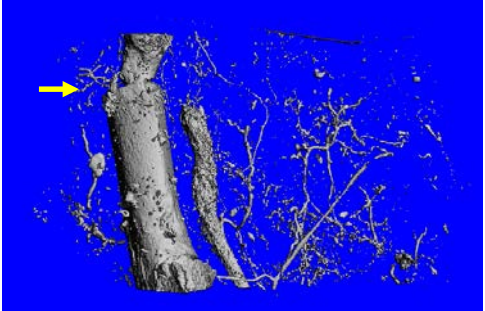
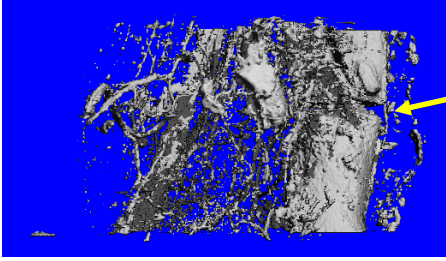
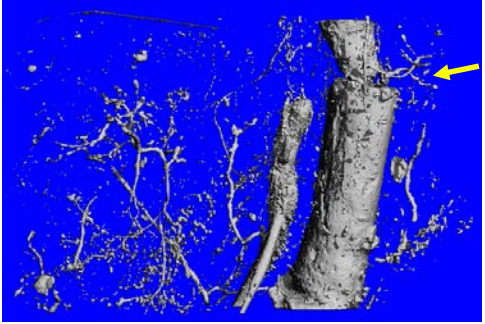
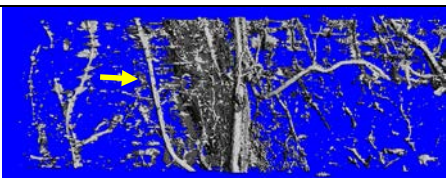
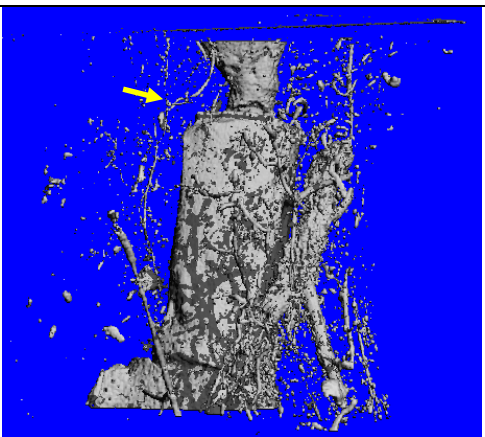
**Figure 20: Barium Perfused Samples.** Both images are from the barium perfusion model. The barium concentration used for both samples was 0.5g/mL. This image portrays the reproducibility across samples.



**Figure 21: Comparison of Barium to Microfil.** The left image is a perfused sample using Microfil as the perfusing agent. The right image is a perfused sample using barium/gelatin as the perfusing agent. The barium model has enhanced vessel resolution to the Microfil, particularly at smaller

Subsequently we repeated our initial results for the comparing BMP2 knockout mice and control mice at day 31. In this study shown in Figure 22, it is obvious that there is more vessel formation in the control than the tamoxifen induced BMP2 knockout. Both femoral arteries and neighboring arterioles are perfused which indicate equivalent amount of perfusion occurred for both samples. The decrease in amount of smaller vessel elements being perfused in these studies now indicates that there is indeed a diminished amount of vessel formation in the conditionally deleted mice consistent now with the mRNA findings.



Rotation	Control	BMP2 Knockout
0°		
90°		
180°		

**Figure 22: Barium Vessel Perfusion for Control Versus BMP2 Knockout.** The control (middle column images) has more vessels compared to the experimental (far right column images). The barium concentration used for both samples was 1.0 g/mL. The rotation angles have no anatomical reference. The yellow arrows indicate the distraction gap.

## DISCUSSION

The x-ray results showed that the femur is healed by day 24, half way into the consolidation phase, for both control and experimental groups. This was verified by the  $\mu$ CT results. The qPCR results for SMA in the femur confirmed that the *Cre/loxP* system works as intended as there is no difference between the control and the experimental. This was further confirmed by BMP2 levels are decreased in the muscle which confirms the fact that the *Cre/loxP* system is working as intended on SMA positive cells. However, BMP2 expression in the distraction gap has no clear distinction between the control and knockout, this might be due to the limited number of SMA positive cells located within the distraction gap.

Most of the BMP2 knockout's bone producing genes in the femur such as RUNX2, osteocalcin, osterix, and BSP from the qPCR results is elevated compared to the control in fold change especially at the late time points. Also, there are raised levels of Cathepsin K in tamoxifen induced BMP2 knockout which suggests higher osteoclast activity. This may explain why there was less bone in the knockout compared to the control shown in the plain X-ray and  $\mu$ CT bone evaluations. Furthermore, earlier formation of cartilage in the femur is depicted by early spikes in expression for Col10a and Acan profiles. This may suggest that the cartilaginous callus appears earlier but is not as large for the knockout due to the differences in peak magnitudes of RNA levels especially for Col10a.

The difference in angiogenesis between muscle and bone is best represented by the ve-cadherin and VEGFR2 gene profiles. It is obvious that angiogenesis in the muscle



decreased as seen in reduced levels for both ve-cadherin and VEGFR2 expression at all time points when tamoxifen was present. This was further validated by diminished levels of expression for both endomucin and Pecam1. However, the level of gene expression for ve-cadherin and VEGFR2 in the bone is not as pronounced as it is in the muscle. The largest difference in magnitude for gene expression between the control and BMP2 knockout for muscle was 5.11 for ve-cadherin, and 2.20 for VEGFR2 at day 17. The bone also had the largest gap between the control and BMP2 knockout at day 17. However, the magnitude of the gap was 2.95 for ve-cadherin, and 1.33 for VEGFR2. Interestingly, ve-cadherin and VEGFR2 levels of expression drastically dropped at day 24 for the femur. This feature was absent in the muscle although the difference diminished slightly at day 24 and day 31. These results suggested that the femur was not as affected by the BMP2 knockout in SMA cells as to the muscle but angiogenesis was slightly inhibited.

When we examined VegfA in the bone, gene expression levels at day 24 was higher for the BMP2 knockout than the control by 1.17 fold. This suggests that the callus is signaling for vessel formation to allow further bone repair as cells and other growth factors outside of the distraction gap are unable to reach the underdeveloped callous. However, since VEGFR2 was reduced at day 17 and only slightly recovered at day 24, the endothelial cells were unable to respond to high levels of VegfA to undergo sprouting angiogenesis.

To further support the idea of reduced angiogenesis,  $\mu$ CT results for the Microfil model showed there is an increase in vessels, especially smaller vessels such as capillaries for the control. Perhaps this suggests a secondary pathway where angiogenesis

occurs as there is a discrepancy in  $\mu$ CT and qPCR. However, this discrepancy was to technical issues as vessels bursting under elevated back pressure it was a common occurrence when using the Microfil model. The issue was resolved when the Microfil model was replaced by the barium/gelatin model. The greatly lower viscosity of the barium/gelatin model produced less pressure as perfusion proceeded which allowed a much greater volume of barium to perfuse the samples compared to the Microfil model. All barium perfused samples had comparable vascular perfusions between specimens because not only was the femoral artery consistently filled but also the larger vessels branching from the femoral artery were visible to the naked eye. This feature was rarely observed when perfusing with Microfil. The barium model undoubtedly showed that there is indeed a decrease in vessels for the tamoxifen induced BMP2 knockout to the control. The  $\mu$ CT bone evaluation data further confirmed a decrease in bone formed in the control than the knockout. Therefore, it seems that when BMP2 is knocked out in SMA cells, it inhibits angiogenesis which then causes a decrease in osteogenesis.

### ***Future Goals***

We hope to continue barium perfusions as the results are very promising due to their consistency and increase in vessels perfused. In addition to our  $\mu$ CT scans, we plan to complete vessel imaging to quantify the total volume of vessels and vessel types to compare the control to the experimental. Also, we plan to finish our  $\mu$ CT bone evaluations with to quantify bone volume data to compare control to tamoxifen-induced BMP2 knockout samples.

Specific studies will also be undertaken to examine additional genes for both femur and muscle environment to capture a more complete picture of how BMP2 deletion in the surrounding muscle, muscle compartments effects angiogenesis. Finally, we will complete the histological analysis to provide further visualization of angiogenesis, chondrogenesis and osteogenesis within the various tissue compartments effected by distraction.

## REFERENCES

- Adams, R. H., & Alitalo, K. (2007). Molecular regulation of angiogenesis and lymphangiogenesis. *Nature Reviews. Molecular Cell Biology*, 8(June), 464–478. doi:10.1038/nrm2183
- Ai-Aql, Z. S., Alagl, a S., Graves, D. T., Gerstenfeld, L. C., & Einhorn, T. a. (2008). Molecular mechanisms controlling bone formation during fracture healing and distraction osteogenesis. *Journal of Dental Research*, 87(2), 107–118. doi:10.1177/154405910808700215
- Aronson, J. (1994). Experimental and clinical experience with distraction osteogenesis. *The Cleft Palate-Craniofacial Journal*. doi:10.1597/1545-1569(1994)031<0473:EACEWD>2.3.CO;2
- Bais, M. V., Wigner, N., Young, M., Toholka, R., Graves, D. T., Morgan, E. F., ... Einhorn, T. a. (2009). BMP2 is essential for post natal osteogenesis but not for recruitment of osteogenic stem cells. *Bone*, 45(2), 254–266. doi:10.1016/j.bone.2009.04.239
- Bi, W., Deng, J. M., Zhang, Z., Behringer, R. R., & de Crombrughe, B. (1999). Sox9 is required for cartilage formation. *Nature Genetics*, 22(may), 85–89. doi:10.1038/8792
- Bragdon, B., Moseychuk, O., Saldanha, S., King, D., Julian, J., & Nohe, A. (2011). Bone Morphogenetic Proteins: A critical review. *Cellular Signalling*, 23(4), 609–620. doi:10.1016/j.cellsig.2010.10.003
- Burri, P. H., Hlushchuk, R., & Djonov, V. (2004). Intussusceptive angiogenesis: Its emergence, its characteristics, and its significance. *Developmental Dynamics*, 231(September), 474–488. doi:10.1002/dvdy.20184
- CDC. (2013). Older Adult Falls - Data and Statistics - Home and Recreational Safety - Injury Center. Retrieved April 2, 2014, from <http://www.cdc.gov/homeandrecreationalafety/Falls/data.html>
- Clarke, B. (2008). Normal Bone Anatomy and Physiology. *Clinical Journal of the American Society of Nephrology : CJASN*, 3(Suppl 3), S131–S139. doi:10.2215/CJN.04151206
- Dienz, O., & Rincon, M. (2010). The effects of IL-6 on CD4 T cell responses. *Clinical Immunology*, 130(1), 27–33. doi:10.1016/j.clim.2008.08.018.The

- Gerhardt, H. (2008). VEGF and endothelial guidance in angiogenic sprouting. *Organogenesis*, 4(March 2015), 241–246. doi:10.4161/org.4.4.7414
- Ghosh, K., & Duyne, G. Van. (2002). Cre–loxP biochemistry. *Methods*, 28, 374–83. Retrieved from <http://www.sciencedirect.com/science/article/pii/S104620230200244X>  
<http://www.ncbi.nlm.nih.gov/pubmed/12431441>
- Haruyama, N., Cho, A., & Kulkarni, A. B. (2010). Overview: Engineering transgenic constructs and mice, 42, 1–12. doi:10.1002/0471143030.cb1910s42.Overview
- Jain, A. P., Pundir, S., & Sharma, A. (2013). Bone morphogenetic proteins: The anomalous molecules. *Journal of Indian Society of Periodontology*, 17(5), 583–586. doi:10.4103/0972-124X.119275
- Kusumbe, A. P., Ramasamy, S. K., & Adams, R. H. (2014). Coupling of angiogenesis and osteogenesis by a specific vessel subtype in bone. *Nature*, 507(7492), 323–8. doi:10.1038/nature13145
- Kyrkanides, S., Miller, J. N. H., Bowers, W. J., & Federoff, H. J. (2003). Transcriptional and posttranslational regulation of Cre recombinase by RU486 as the basis for an enhanced inducible expression system. *Molecular Therapy*, 8(5), 790–795. doi:10.1016/j.ymthe.2003.07.005
- Lichtman, a H., Chin, J., Schmidt, J. a, & Abbas, a K. (1988). Role of interleukin 1 in the activation of T lymphocytes. *Proceedings of the National Academy of Sciences of the United States of America*, 85(December), 9699–9703.
- Lissenberg-Thunnissen, S. N., De Gorter, D. J. J., Sier, C. F. M., & Schipper, I. B. (2011). Use and efficacy of bone morphogenetic proteins in fracture healing. *International Orthopaedics*, 35(9), 1271–1280. doi:10.1007/s00264-011-1301-z
- Livak, K. J., & Schmittgen, T. D. (2001). Analysis of relative gene expression data using real-time quantitative PCR and the 2(-Delta Delta C(T)) Method. *Methods (San Diego, Calif.)*, 25, 402–408. doi:10.1006/meth.2001.1262
- Lu, C., Marcucio, R., & Miclau, T. (2006). Assessing angiogenesis during fracture healing. *The Iowa Orthopaedic Journal*, 26, 17–26.
- Lybrand, K., Bragdon, B., & Gerstenfeld, L. (2015). Mouse models of bone healing: fracture, marrow ablation, and distraction osteogenesis. *Current Protocols in Mouse Biology*, 5(1), 35–49. doi:10.1002/9780470942390.mo140161

- Mackie, E. J., Ahmed, Y. a., Tatarczuch, L., Chen, K. S., & Mirams, M. (2008). Endochondral ossification: How cartilage is converted into bone in the developing skeleton. *International Journal of Biochemistry and Cell Biology*, 40, 46–62. doi:10.1016/j.biocel.2007.06.009
- Makhdom, A. M., & Hamdy, R. C. (2013). The role of growth factors on acceleration of bone regeneration during distraction osteogenesis. *Tissue Engineering. Part B, Reviews*, 19(5), 442–53. doi:10.1089/ten.TEB.2012.0717
- Marsell, R., & Einhorn, T. a. (2011). The biology of fracture healing. *Injury*, 42(6), 551–555. doi:10.1016/j.injury.2011.03.031
- Matsubara, H., Hogan, D. E., Morgan, E. F., Mortlock, D. P., Einhorn, T. a., & Gerstenfeld, L. C. (2012). Vascular tissues are a primary source of BMP2 expression during bone formation induced by distraction osteogenesis. *Bone*, 51(1), 168–180. doi:10.1016/j.bone.2012.02.017
- Mescher, A. (2013). *Junqueira's Basic Histology: Text & Atlas* (13th ed., pp. 138–159). New York, NY: McGraw Hill.
- Morgan, E. F., Hussein, A. I., Al-Awadhi, B. a., Hogan, D. E., Matsubara, H., Al-Alq, Z., ... Gerstenfeld, L. C. (2012). Vascular development during distraction osteogenesis proceeds by sequential intramuscular arteriogenesis followed by intraosteal angiogenesis. *Bone*, 51(3), 535–545. doi:10.1016/j.bone.2012.05.008
- Natu, S. S., Ali, I., Alam, S., Giri, K. Y., Agarwal, A., & Kulkarni, V. A. (2014). The biology of distraction osteogenesis for correction of mandibular and craniomaxillofacial defects: A review. *Dental Research Journal*, 11(1), 16–26. Retrieved from <http://www.ncbi.nlm.nih.gov/pubmed/24688555>
- Ogasawara, T., Kawaguchi, H., Jinno, S., Hoshi, K., Itaka, K., Takato, T., ... Okayama, H. (2004). Bone morphogenetic protein 2-induced osteoblast differentiation requires Smad-mediated down-regulation of Cdk6. *Molecular and Cellular Biology*, 24(15), 6560–6568. doi:10.1128/MCB.24.15.6560-6568.2004
- Otrock, Z. K., Mahfouz, R. a R., Makarem, J. a., & Shamseddine, A. I. (2007). Understanding the biology of angiogenesis: Review of the most important molecular mechanisms. *Blood Cells, Molecules, and Diseases*, 39, 212–220. doi:10.1016/j.bcmd.2007.04.001
- Parums, D. V., Cordell, J. L., Micklem, K., Heryet, A. R., Gatter, K. C., & Mason, D. Y. (1990). JC70: a new monoclonal antibody that detects vascular endothelium associated antigen on routinely processed tissue sections. *Journal of Clinical*

- Pathology*, 43(9), 752–757. Retrieved from <http://www.ncbi.nlm.nih.gov/pmc/articles/PMC502755/>
- Pechisker, A. (2004). TARGETING YOUR DNA WITH THE CRE/LOX SYSTEM | SCQ. Retrieved February 16, 2015, from <http://www.scq.ubc.ca/targeting-your-dna-with-the-crelox-system/>
- Percival, C. J., & Richtsmeier, J. T. (2013). Angiogenesis and Intramembranous Osteogenesis. *Developmental Dynamics : An Official Publication of the American Association of Anatomists*, 242(8), 909–922. doi:10.1002/dvdy.23992
- Roche, B., David, V., Vanden-Bossche, A., Peyrin, F., Malaval, L., Vico, L., & Lafage-Proust, M. H. (2012). Structure and quantification of microvascularisation within mouse long bones: What and how should we measure? *Bone*, 50(1), 390–399. doi:10.1016/j.bone.2011.09.051
- Shidara, K., Inaba, M., Okuno, S., Yamada, S., Kumeda, Y., Imanishi, Y., ... Nishizawa, Y. (2008). Serum levels of TRAP5b, a new bone resorption marker unaffected by renal dysfunction, as a useful marker of cortical bone loss in hemodialysis patients. *Calcified Tissue International*, 82, 278–287. doi:10.1007/s00223-008-9127-4
- Shu, B., Zhang, M., Xie, R., Wang, M., Jin, H., Hou, W., ... Chen, D. (2011). BMP2, but not BMP4, is crucial for chondrocyte proliferation and maturation during endochondral bone development. *Journal of Cell Science*, 124, 3428–3440. doi:10.1242/jcs.083659
- Takayanagi, H. (2007). Osteoclast differentiation and activation. *Clinical Calcium*, 17(May), 484–492. doi:10.1038/nature01658
- Ueno, M., Igarashi, K., Kimura, N., Okita, K., Takizawa, M., Nobuhisa, I., ... Taga, T. (2001). Endomucin is expressed in embryonic dorsal aorta and is able to inhibit cell adhesion. *Biochemical and Biophysical Research Communications*, 287, 501–506. doi:10.1006/bbrc.2001.5587
- Venkiteswaran, K., Xiao, K., Summers, S., Calkins, C. C., Vincent, P. a, Pumiglia, K., & Kowalczyk, A. P. (2002). Regulation of endothelial barrier function and growth by VE-cadherin, plakoglobin, and beta-catenin. *American Journal of Physiology. Cell Physiology*, 283, C811–C821. doi:10.1152/ajpcell.00417.2001
- Wigner, N. a., Soung, D. Y., Einhorn, T. a., Drissi, H., & Gerstenfeld, L. C. (2013). Functional role of Runx3 in the regulation of aggrecan expression during cartilage development. *Journal of Cellular Physiology*, 228(April), 2232–2242. doi:10.1002/jcp.24396

Yang, W., Guo, D., Harris, M. A., Cui, Y., Gluhak-heinrich, J., Wu, J., ... Harris, S. E. (2012). Bmp2 in osteoblasts of periosteum and trabecular bone links bone formation to vascularization and mesenchymal stem cells. doi:10.1242/jcs.118596



## CURRICULUM VITAE

THOMAS W. CHENG

### Personal Information

Current Address: 202 Orient Ave., Floor 3, Boston, MA, 02128, USA

Permanent Address: 5104 Harbourview Road, Burnaby, BC, v5b1c8, Canada

Email: twtcheng@bu.edu

Phone: 443-813-0262

Year of Birth: 1991

### Education

**Boston University School of Medicine** Boston, MA  
Candidate for Master of Sciences for Medical Sciences Expected May, 2015  
Relevant Coursework: Biochemistry and Cell Biology, Cellular Organization of Tissue,  
Introduction to Pathology, Advanced Human Physiology

**Johns Hopkins University** Baltimore, MD  
Bachelor of Science in Chemical & Biomolecular Engineering May, 2013

### Research Experience

**Gerstenfeld Lab at Boston University** Boston, MA  
Graduate Researcher July, 2014 – May, 2015

- Worked with mice to determine the role of BMP2 for bone repair during distraction osteogenesis
- Used X-ray, micro computerized tomography, vessel perfusion, and microbiology techniques to elucidate the mechanism of BMP2
- Presented findings at 2015 Graduate Research Symposium and published abstracts in the 2015 MAMS Research Symposium Program

**Wirtz Lab at Johns Hopkins University** Baltimore, MD  
Undergraduate Researcher November, 2010 – May, 2013

- Worked with breast and lung cancer cells for single cell phenotyping and tumor growth
- Learned cell culture techniques, simple microscopy, and data analysis using MATLAB
- Presented research work in a lab meeting and trained new undergraduates cell culture techniques

- Ostermeier Lab at Johns Hopkins University** Baltimore, MD  
Undergraduate Researcher March, 2010 – September, 2010
- Worked with E.Coli to investigate protein evolution through band-pass systems
  - Learned molecular biology techniques such as Western Blotting, MiniPrep, inoculation, transformation, gel electrophoresis, PCR

### **Medically Related Experience**

- Boston Medical Center** Boston, MA  
Volunteer Ambassador March - November, 2014
- Enhanced patients' experiences at the hospital by welcoming them and giving directions to their appointments
  - Escorted patients to their appointments when they were unfamiliar with the hospital or needed further assistance

- Practicum in Orthopedic & Shoulder Surgery** Baltimore, MD  
Shadowing Dr. Edward McFarland January – May, 2013
- Observed shoulder arthroscopy, open shoulder surgery, and reverse shoulder replacement surgery at Zayed Tower in Johns Hopkins Hospital
  - Observed doctor-patient interactions in the Greenspring Station Clinic as well as helped doctors administer cortisone shots

- Introduction to the Operating Room and Anesthesia** Baltimore, MD  
Shadowing Dr. A.D. John January – December, 2012
- Observed a variety of surgeries such as gastric bypass, breast reduction, knee replacement, and cardiovascular operations at Johns Hopkins Bayview Hospital
  - Observed patients in PACU and became accustomed to the environment in the OR (ie: blue is sterile)

- Global Medical Brigade** Rapaco, Honduras  
Volunteer January, 2011
- Performed triage and shadowed physicians
  - Provided medical relief, prescriptions, and over-the-counter medication to local villagers

### **Achievements**

Dean's List for Fall Semester 2011 at Johns Hopkins University

### **Work Experience**

**Burnaby Tennis Club** Burnaby, BC

Tennis Instructor and Volunteer

June – August, 2006 – 2009

- Taught groups of 4 to 5 children at beginner level to play tennis
- Organized and managed the Burnaby Open 2008 tournament
- Volunteered at additional summer camps to assist coaches in teaching